2007-08-28

A Comparison of Optimized Nonlinear Time History Analysis and the Equivalent Lateral Forces Method for Brace Design

Lukas Balling
Brigham Young University - Provo

DESIGN OF BUCKLING-RESTRAINED BRACED FRAMES USING NONLINEAR TIME HISTORY ANALYSIS AND OPTIMIZATION

by

Lukas J. Balling

A thesis submitted to the faculty of

Brigham Young University

in partial fulfillment of the requirements for the degree of

Master of Science

Department of Civil and Environmental Engineering

Brigham Young University

December 2007

BRIGHAM YOUNG UNIVERSITY

GRADUATE COMMITTEE APPROVAL

of a thesis submitted by

Lukas J Balling

This thesis has been read by each member of the following graduate committee and by majority vote has been found to be satisfactory.

Date	Richard J. Balling, Chair
Date	Paul W. Richards
Date	Fernando S. Fonseca

BRIGHAM YOUNG UNIVERSITY

As chair of the candidate's graduate committee, I have read the thesis of Lukas J. Balling in its final form and have found that (1) its format, citations, and bibliographical style are consistent and acceptable and fulfill university and department style requirements; (2) its illustrative materials including figures, tables, and charts are in place; and (3) the final manuscript is satisfactory to the graduate committee and is ready for submission to the university library.

Date

Richard J. Balling
Chair, Graduate Committee

Accepted for the Department

E. James Nelson
Graduate Coordinator

Accepted for the College

Alan R. Parkinson
Dean, Ira A. Fulton College of Engineering and Technology

ABSTRACT

DESIGN OF BUCKLING-RESTRAINED BRACED FRAMES USING NONLINEAR TIME HISTORY ANALYSIS AND OPTIMIZATION

Lukas J. Balling

Department of Civil and Environmental Engineering

Master of Science

This thesis presents the development of a design procedure for buckling-restrained braced frames (BRBF's). This procedure uses nonlinear time history analysis and a formal optimization algorithm. The time history analysis includes an elasto-plastic model for the braces. The optimization algorithm is a genetic algorithm. This procedure is referred to throughout the thesis as the "Nonlinear Time History Analysis Procedure with Optimization" (NTHO).

Current design specifications for BRBF's are based on inelastic design spectra and approximate formulas for the determination of natural period. These spectra are used to obtain seismic base shear, and the distribution of equivalent lateral forces. Yielding and

drift criteria are then used to determine brace areas. This design procedure is referred to throughout the thesis as the "Equivalent Lateral Force Procedure" (ELF).

The thesis compares results from the NTHO and ELF procedures for a variety of BRBF's and levels of seismicity. The ELF procedure is judged against the more accurate NTHO procedure, and BRBF's are identified where the ELF procedure produces unconservative and excessively conservative designs.

Since the NTHO procedure is more computationally expensive than the ELF procedure, design charts are developed for quickly sizing brace areas for a variety of BRBF's based on the NTHO procedure. Among the conclusions at the end of the thesis is the surprising result that the design charts show a near linear variation of brace area from story to story.

ACKNOWLEDGMENTS

I would like to thank Professor Richard J. Balling, Professor Paul W. Richards, and Professor Fernando S. Fonseca for all of the help and knowledge that they have given me. They are pillars of wisdom in the Civil Engineering Department at BYU. I would especially like to thank my father, Professor Richard J. Balling, for helping me throughout the years to finally become a structural engineer. Also, I would like to thank my beautiful wife, Melinda, for all of the support that she has given me.

TABLE OF CONTENTS

LIST OF TABLES ..... **ix**

LIST OF FIGURES ..... **xi**

1 Introduction **1**

2 Previous Research **5**

3 Equivalent Lateral Force Procedure **9**

3.1 Construct Design Response Spectrum 9

3.2 Estimate the Fundamental Period 10

3.3 Determine Seismic Base Shear 11

3.4 Distribute the Story Forces 12

3.5 Conduct Static Analysis 13

3.6 Determine Brace Area 15

4 Nonlinear Time History Procedure with Optimization **17**

4.1 Structural Model 17

4.1.1 Stress and Strain 19

4.1.2 Stiffness Matrix 20

4.1.3 Resistance Vector 21

4.1.4 Force Vector 21

4.1.5 Mass Matrix 22

4.1.6 Damping Matrix 23

4.2 Nonlinear Response History Analysis 24

4.3 Optimization 28

5 Consistent Input and Output Parameters 37

5.1 Mass Independence 38

5.2 Variable Input Parameters 39

5.3 Consistent Accelerogram Scale Factors 39

5.4 Consistent Allowable Ductility 48

5.5 Consistent Allowable Drift 49

5.6 Consistent Yield Stress 49

5.7 Consistent ϕ Factor 50

6 Results 51

6.1 Comparison Graphs 51

6.2 Controlling Constraint Tables 58

6.3 Design Charts 61

7 Conclusion 75

References 77

LIST OF TABLES

Table 5-1 Scale Factors....48

Table 6-1 One-Story S_{DS}=1.2....58

Table 6-2 One-Story S_{DS}=0.9....59

Table 6-3 One-Story S_{DS}=0.6....59

Table 6-4 Three-Story S_{DS}=1.2....59

Table 6-5 Three-Story S_{DS}=0.9....59

Table 6-6 Three-Story S_{DS}=0.6....60

Table 6-7 Five-Story S_{DS}=1.2....60

Table 6-8 Five-Story S_{DS}=0.9....60

Table 6-9 Five-Story S_{DS}=0.6....60

LIST OF FIGURES

Figure 1-1 Planar Braced Frame 1

Figure 3-1 Response Spectrum 11

Figure 3-2 Free-Body Diagram 14

Figure 4-1 Structural Model 18

Figure 4-2 Elasto-plastic Stress and Strain 19

Figure 5-1 Accelerogram 1 41

Figure 5-2 Accelerogram 2 41

Figure 5-3 Accelerogram 3 41

Figure 5-4 Accelerogram 4 42

Figure 5-5 Accelerogram 5 42

Figure 5-6 Accelerogram 6 42

Figure 5-7 Accelerogram 7 43

Figure 5-8 Accelerogram 8 43

Figure 5-9 Accelerogram 9 43

Figure 5-10 Accelerogram 10 44

Figure 5-11 Pseudo-Acceleration 1 44

Figure 5-12 Pseudo-Acceleration 2 44

Figure 5-13 Pseudo-Acceleration 3 45

Figure 5-14 Pseudo-Acceleration 4 45

Figure 5-15 Pseudo-Acceleration 5 45

Figure 5-16 Pseudo-Acceleration 6 46
Figure 5-17 Pseudo-Acceleration 7 46
Figure 5-18 Pseudo-Acceleration 8 46
Figure 5-19 Pseudo-Acceleration 9 47
Figure 5-20 Pseudo-Acceleration 10 47
Figure 5-21 Ductility Ratio Diagram (FEMA 450, 2003) 49
Figure 5-22 BRB Overstrength (Coy, 2007)....50
Figure 6-1 One-Story S_{DS}=1.2 A/m 52
Figure 6-2 One-Story S_{DS}=0.9 A/m 53
Figure 6-3 One-Story S_{DS}=0.6 A/m 53
Figure 6-4 Three-Story S_{DS}=1.2 A/m 54
Figure 6-5 Three-Story S_{DS}=0.9 A/m 54
Figure 6-6 Three-Story S_{DS}=0.6 A/m 55
Figure 6-7 Five-Story S_{DS}=1.2 A/m....55
Figure 6-8 Five-Story S_{DS}=0.9 A/m....56
Figure 6-9 Five-Story S_{DS}=0.6 A/m....56
Figure 6-10 One-Story Design Chart....62
Figure 6-11 One-Story Design Chart....62
Figure 6-12 One-Story Design Chart....63
Figure 6-13 Three-Story Design Chart 63
Figure 6-14 Three-Story Design Chart 64
Figure 6-15 Three-Story Design Chart 64
Figure 6-16 Three-Story Design Chart 65
Figure 6-17 Three-Story Design Chart 65
Figure 6-18 Three-Story Design Chart 66

Figure 6-19 Three-Story Design Chart 66
Figure 6-20 Three-Story Design Chart 67
Figure 6-21 Three-Story Design Chart 67
Figure 6-22 Three-Story Design Chart 68
Figure 6-23 Three-Story Design Chart 68
Figure 6-24 Five-Story Design Chart 69
Figure 6-25 Five-Story Design Chart 69
Figure 6-26 Five-Story Design Chart 70
Figure 6-27 Five-Story Design Chart 70
Figure 6-28 Five-Story Design Chart 71
Figure 6-29 Five-Story Design Chart 71
Figure 6-30 Five-Story Design Chart 72
Figure 6-31 Five-Story Design Chart 72
Figure 6-32 Five-Story Design Chart 73

1 Introduction

This thesis treats the design of planar Buckling-Restrained Braced Frames (BRBF's) frames such as those shown in Figure 1-1. It is assumed that all stories have the same story height H, mass m, and all bays have the same bay width L. It is assumed that all connections are hinged (shear) connections.

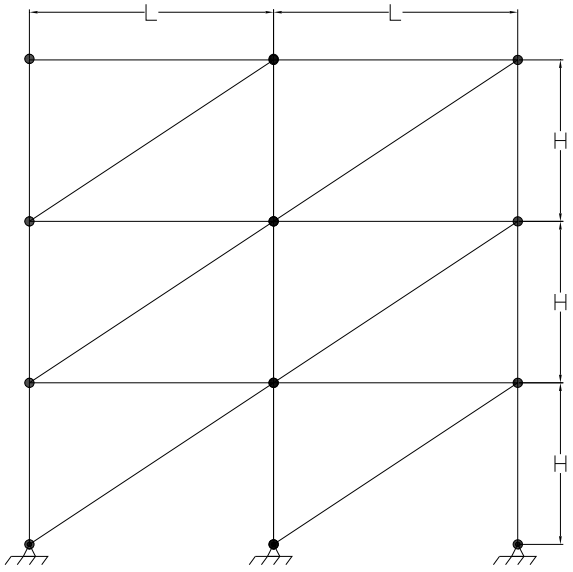

Figure 1-1 Planar Braced Frame

BRBF's were developed to prevent undesirable post buckling behavior under earthquake loading. Commonly-used special concentric braces are known to have undesirable behavior due to loss of strength and stiffness after braces buckle in

compression (SEAOC, 1999). Buckling-restrained braces (BRB's) consist of a steel core that deforms in-elastically under strong earthquake loads, that is surrounded by an outer casing that restrains local buckling. Also, BRB's are approximately 1.1 times stronger under compression loading than tension loading (Tremblay, 2006). This allows a BRB to resist lateral forces with both tension and compression rather than with tension only as in the case of a concentric brace.

Most braced frames are designed using the Equivalent Lateral Force (ELF) procedure specified by the 2003 edition of FEMA 450 and the 2005 edition of ASCE-7. This procedure is a very fast and economical design method. The same codes and provisions also allow a Nonlinear Time History (NTH) procedure for the design of braced frames. The NTH procedure gives a more accurate model of seismic forces than the ELF procedure, however; it is more time-consuming and is not widely used in practice.

The cross-sectional areas of the braces in a braced frame dramatically affect the material cost of the building. This is because braces must be designed to yield before the columns and girders in order to prevent catastrophic failure under strong earthquake loading. A decrease in brace area may make it possible to significantly decrease the areas of the columns and girders. Therefore, it is very desirable to optimize the cross-sectional brace areas.

The goals of this research are: 1) develop a procedure (NTHO) for the design of BRBF's based on formal optimization and the NTH analysis procedure; 2) compare designs obtained with the ELF procedure to designs obtained with the NTHO procedure on BRBF's with varying number of stories, story heights, and bay lengths; 3) create

design charts from the results for the NTHO procedure that can be used for fast design of brace areas in BRBF's.

This thesis first discusses previous research on the analysis, design, and optimization of BRBF's and steel frames in general. The next two chapters present the ELF and NTHO procedures, respectively. Consistent input parameters are then determined in order to ensure that the two procedures are properly compared. Results from both procedures are presented and compared, and design charts are developed from the NTHO procedure. Finally, conclusions and recommendations are submitted.

2 Previous Research

BRB's have been under study for the last 30 years. One of the first studies that proved that BRB's were a viable form of resisting earthquake loadings was done by Watanabe, A. and Hitomoi, Y. (1988). They tested BRB's where hollow steel tubes were used as the brace outer casing. In their study they showed that the outer casings of various brace lengths were effective in preventing buckling of the steel core. Later Trembley, R. and Buldoc, P. (2006) tested two different buckling-restraining mechanisms (concrete-filled tubes and hollow steel tubes) and found that both mechanisms demonstrated an adequate ductile seismic response.

Sabelli, R.; Mahin, S.; and Chang, C. (2003) performed a nonlinear time history analysis on three-story and six-story BRBF's and special concentric braced frames with braces in a chevron and two-story X patterns. They determined that buckling-restrained braces provide an effective means for overcoming the potential problems associated with special concentric braced frames under seismic loads.

Black, C. and Makris, N. (2004) determined, through a comprehensive experimental program, that BRB's deliver ductile, stable, and repeatable hysteretic behavior. Also, they determined that the plastic deformation capacity of the braces exceeded specific requirements for ultimate deformation and cumulative plastic strain. Furthermore, in their research they performed a nonlinear time history analysis and found

that BRB's are capable of providing the rigidity required to satisfy structural drift limits while displaying stable energy absorption capabilities.

Kiggins, S. and Uang, C. (2006) performed a nonlinear time history analysis on three-story and five-story BRBF's that were used in a dual system or where the frame had moment beam-column connections with BRB's. They found that the residual drifts decreased in dual system BRBF's from regular BRBF's systems.

Many studies have developed design methods for buckling-restrained braces. Kim, J. and Choi, H. (2004) developed and investigated a design procedure for BRBF's based on displacement and a static pushover analysis. They checked this design method with nonlinear time history analysis. Kim, J. and Seo, Y. (2004) proposed a design procedure for the design of low rise structures with BRBF's using a similar design method. Their design method was also based on displacement and a static pushover analysis, but they used scaling factors to better represent forces that were developed from a nonlinear time history analysis.

BRBF's were first introduced into US design practice in 1999. Since then structural design provisions have been developed and adopted by the 2005 edition of the AISC *Seismic Provisions for Structural Steel Buildings* (AISC 341). Sabelli, R. and Pottebaum, W. (2005) demonstrated an optimized design method for the design of buckling-restrained braced frames using the 2005 AISC Seismic Provisions. There design method showed the optimal material input parameters and how to most effectively us the AISC 341 seismic provisions for BRBF's.

Although few researchers have applied optimization methods to the design of BRBF's, there are several studies applying optimization methods to the design of steel

frames, both moment-resisting and braced. Pezeshk, S. (1998) used an optimization algorithm based on optimality criterion approach with constraints on drift to optimize two-story moment-resisting frames. This research compared linear and nonlinear analyses and showed how nonlinear analysis affected the optimum frame designs. Xu, L.; Gong, Y.; and Grierson, D. (2007) performed optimization on three and five-story moment-resisting frames. They used a gradient based optimization and used constraints on drift and ductility. Their optimization also used nonlinear analysis.

Memari, A. M. (1999) used a gradient based optimization algorithm to optimize multi-story braced frames. His study used nonlinear finite element analysis to determine optimum brace areas.

Kameshki and Saka (2001) used a genetic algorithm to optimize different brace pattern designs for a three bay 15-story braced framed structure under seismic forces. Pezeshk, Camp, and Chen (2000) used a genetic algorithm to optimize moment-resisting framed structures using nonlinear analysis. Hayalioglu, M. S. and Degertekin, S.O. also used a genetic algorithm to optimize moment resisting frames. The used a nonlinear analysis and accounted for P-Δ effects in there study.

3 Equivalent Lateral Force Procedure

The Equivalent Lateral Force procedure is used to determine the brace cross-sectional areas through the following six steps:

1) Construct design response spectrum;

2) Estimate the fundamental period of the structure;

3) Determine the seismic base shear;

4) Distribute the vertical seismic forces on each story;

5) Conduct static analysis to determine story drifts and brace axial forces;

6) Determine the brace areas.

3.1 Construct Design Response Spectrum

The design response spectrum prescribed by the Equivalent Lateral Force procedure is shown in Figure 3-1 and depends on five parameters: T_0, T_S, T_L, S_{DS}, and S_{D1}. The parameters S_{DS} and S_{D1} are the design acceleration parameters for short period and one second period, respectively. These parameters depend on the seismicity of the site, the soil properties of the site, and the assumed damping ratio. The USGS developed seismicity maps of the United States for specific damping ratios. From these maps values

are obtained for mapped acceleration parameters S_S and S_1. Then S_{DS} and S_{D1} are calculated from Equations 3.1and 3.2.

$$S_{DS} = \frac{2}{3} F_a S_S \tag{3.1}$$

$$S_{D1} = \frac{2}{3} F_v S_1 \tag{3.2}$$

where the parameters F_a and F_v are read from tables according to the site class for the soil.

The parameter T_L depends on location and is obtained from maps prepared by the USGS. The parameters T_0 and T_S are then calculated using Equations 3.3 and 3.4.

$$T_0 = \frac{0.2 S_{D1}}{S_{DS}} \tag{3.3}$$

$$T_S = \frac{S_{D1}}{S_{DS}} \tag{3.4}$$

3.2 Estimate the Fundamental Period

The fundamental period depends on the stiffness and mass of the structure. The stiffness of the structure depends on the brace areas that have not yet been determined. Therefore, the Equivalent Lateral Force procedure provides an approximate equation for estimating the fundamental period in Equation 3.5.

$$T = C_u C_r (nH)^x \tag{3.5}$$

where C_r and x depend on the structure type, n is the number of stories, H is the story height in feet, and C_u is a coefficient greater than or equal to one that is obtained from a table based on the value of S_{D1}. For BRBF's, $C_r = 0.03$ and $x = 0.75$.

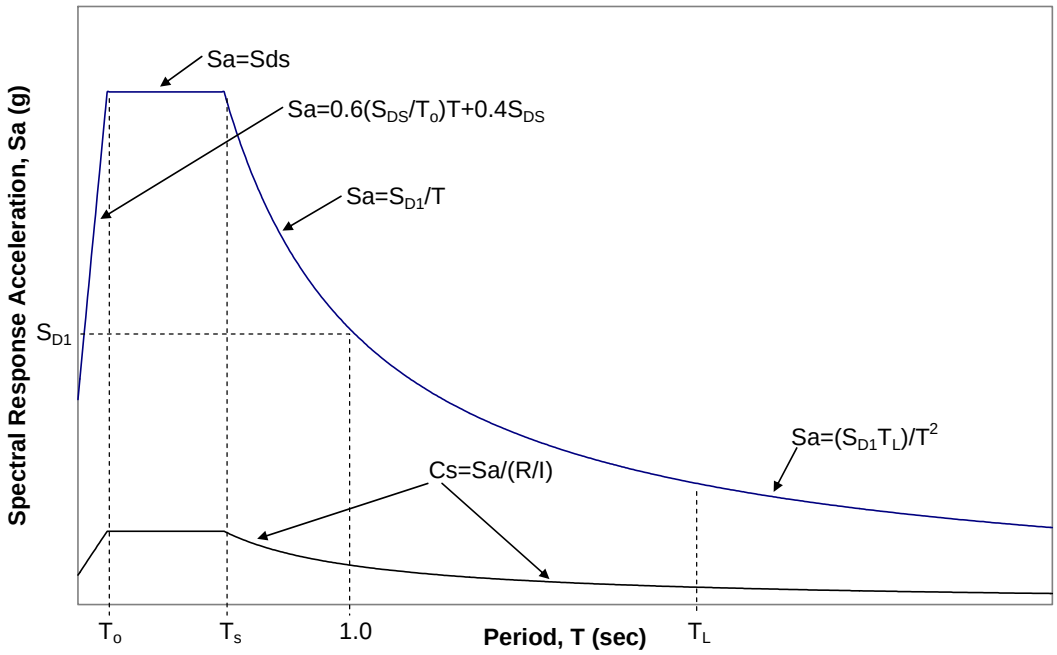

Figure 3-1 Response Spectrum

3.3 Determine Seismic Base Shear

The seismic base shear is the equivalent lateral force applied at the base of the structure and is calculated using Equation 3.6.

$$V = C_S W = C_S nmg \tag{3.6}$$

where W is the total building weight, m is the mass of a single story, n is the number of stories in the structure, and C_S is the seismic response coefficient calculated by Equation 3.7.

$$C_S = \frac{S_a}{R/I} \tag{3.7}$$

where S_a is the spectral response acceleration read from the design response spectrum shown in Figure 3-1 for the fundamental period T. The parameters R and I are the response modification factor and occupancy importance factor, respectively. The response modification factor is based on the structure type. For BRBF's, R = 7. The occupancy importance factor is greater for large buildings with higher occupancies. The parameter C_S shall not be taken less than 0.01, and where S_1 is equal to or greater than 0.6g, C_S shall not be taken less than that calculated by Equation 3.8.

$$C_S = \frac{0.5S_1}{R/I} \tag{3.8}$$

3.4 Distribute the Story Forces

The equivalent lateral story forces, F_i, are determined from the lumped story weights, w_i, and the story heights, h_i, where i ranges from 1 to n = number of stories with i = 1 being the top story and i = n being the bottom story. The lumped story weights must

add up to the total weight W, and the equivalent lateral story forces must add up to the base shear V. The story forces are calculated by Equation 3.9.

$$F_i = \frac{w_i h_i^k}{\sum_{j=1}^{n} w_j h_j^k} V = \frac{mg(n-i+1)^k H^k}{\sum_{j=1}^{n} mg(n-j+1)^k H^k} V = \frac{(n-i+1)^k}{\sum_{j=1}^{n} (n-j+1)^k} V = \frac{2(n-i+1)^k}{n(n+1)} V \quad (3.9)$$

The parameter k depends on the fundamental period T. For T less than or equal to 0.5s, k is equal to 1. For T greater than or equal to 2.5s, k equal to 2. For T between 0.5s and 2.5s, k is equal to 0.75+T/2.

3.5 Conduct Static Analysis

A static analysis is conducted to determine the axial forces in the braces and the horizontal drifts in the stories. It is assumed that all connections are hinged (shear) connections, and that there are no rigid (moment) connections in the frame. A free-body diagram of the top three stories of a multi-story frame is shown in Figure 3-2.

Equation 3.10 provides a formula for calculating the brace force, F_{b3}.

$$F_{b3} = (F_1 + F_2 + F_3)\frac{\sqrt{L^2 + H^2}}{L} \quad (3.10)$$

where H is the story height and L is the story width.

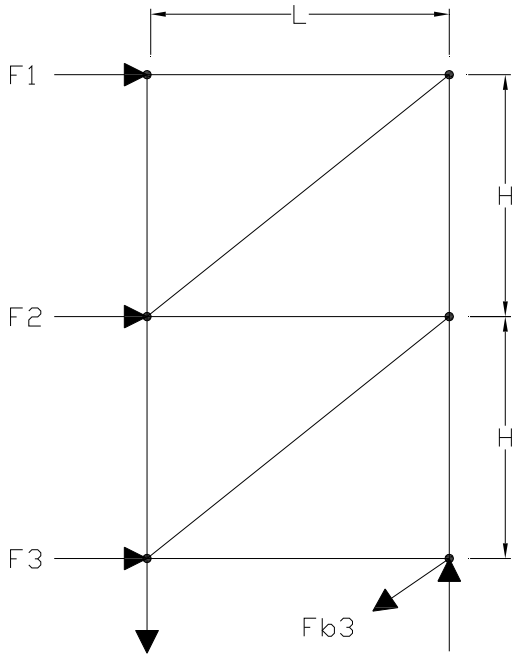

Figure 3-2 Free-Body Diagram

The axial force in the brace at story i is calculated using Equation 3.11.

$$F_{bi} = \left(\sum_{j=1}^{i} F_j \right) \frac{\sqrt{L^2 + H^2}}{L} \tag{3.11}$$

where it is assumed that the axial stiffnesses of the columns and girders are much greater than the axial stiffnesses of the braces.

This assumption leads to the story stiffness given in Equation 3.12.

$$k_i = \frac{A_i E L^2}{(L^2 + H^2)^{3/2}} \tag{3.12}$$

where E is Young's modulus of elasticity and A_i is the cross-sectional area of the brace in story i.

The elastic drift, δ_i, and inelastic drift, Δ_i, at story i are calculated using Equations 3.13 and 3.14.

$$\delta_i = \left(\frac{\sum_{j=1}^{i} F_j}{k_i} \right) \tag{3.13}$$

$$\Delta_i = \frac{C_d \delta_i}{I} \tag{3.14}$$

where C_d is the deflection amplification factor which is determined based on structure type and accounts for inelastic deflections in the structure, and I is the occupancy importance factor. For BRBF's, $C_d = 5.5$.

3.6 Determine Brace Area

Two criteria govern the determination of the brace area in each story. These are yielding and drift. Both can be formulated as inequalities. The yielding criterion for story i is given in Equation 3.15.

$$F_{bi} \leq \phi A_i F_y \tag{3.15}$$

where F_y is the material yield strength and ϕ is a safety factor equal to 0.9.

Substituting Equation 3.11 into Equation 3.15 and solving for the cross-sectional area gives Equation 3.16.

$$A_i \geq \left(\sum_{j=1}^{i} F_j \right) \frac{\sqrt{L^2 + H^2}}{L \phi F_y} \tag{3.16}$$

The drift criterion for story i is given in Equation 3.17.

$$\Delta_i \leq C_{Drift} H \tag{3.17}$$

where C_{Drift} is 0.02 for frames with five or more stories and 0.025 for frames with four or less stories.

Substituting Equations 3.12, 3.13, and 3.14 into Equation 3.17, the cross-sectional area can be calculated in Equation 3.18.

$$A_i \geq \left(\sum_{j=1}^{i} F_j \right) \frac{C_d (L^2 + H^2)^{3/2}}{I C_{Drift} H E L^2} \tag{3.18}$$

Equations 3.16 and 3.18 are then evaluated to determine story cross-sectional area.

4 Nonlinear Time History Procedure with Optimization

The Nonlinear Time History procedure with optimization differs from the Equivalent Lateral Force procedure in two respects. First, time history analysis with elasto-plastic braces is used rather than response spectra analysis. Second, an optimization procedure is used to determine brace areas rather than approximating the fundamental natural period with a formula that is independent of brace area. The nonlinear time history analysis and optimization procedures are described in this chapter.

4.1 Structural Model

The structural model consists of a horizontal displacement degree-of-freedom, u_i, at each story i where i = 1 is the top story and i = n is the bottom story as shown in Figure 4-1. The equations of motion is given in Equation 4.1.

$$M\ddot{U} + C\dot{U} + R = F \tag{4.1}$$

where **M** is the mass matrix, **C** is the damping matrix, **R** is the resistance vector, **F** is the force vector, **U** is the displacement vector, $\dot{\mathbf{U}}$ is the velocity vector, and $\ddot{\mathbf{U}}$ is the acceleration vector.

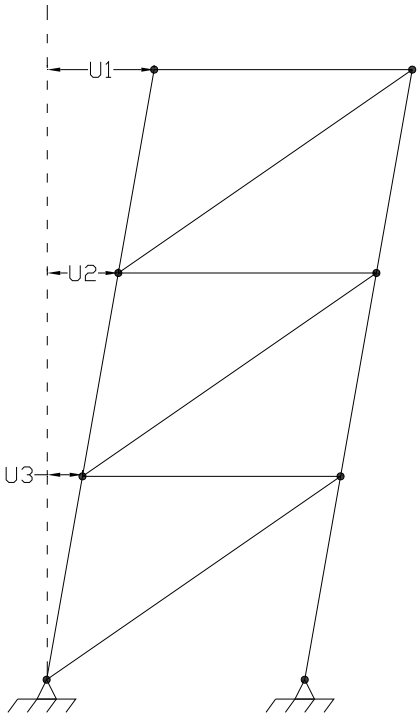

Figure 4-1 Structural Model

The resistance vector is a nonlinear function of the displacement vector, however; a linear approximation of the resistance vector in the vicinity of the current displacement vector $\mathbf{U}^*$ is shown in Equations 4.2 and 4.3.

$$\mathbf{R} \approx \mathbf{R}^* + \mathbf{K}^* \Delta \mathbf{U} \tag{4.2}$$

$$\Delta \mathbf{U} = \mathbf{U} - \mathbf{U}^* \tag{4.3}$$

4.1.1 Stress and Strain

It is assumed that the behavior of BRB's is the same in tension and compression, and that the behavior is elastic-perfectly-plastic (elasto-plastic) as shown in Figure 4-2.

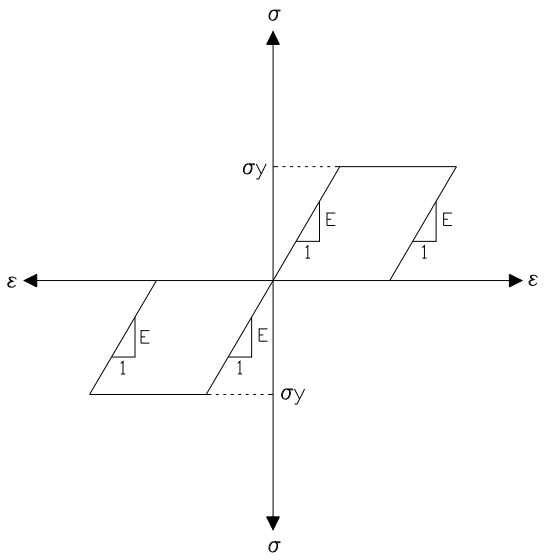

Figure 4-2 Elasto-plastic Stress and Strain

The current strain in the braces of story i is given in Equation 4.4.

$$\varepsilon_i^* = \frac{L}{L^2 + H^2}\left(u_i^* - u_{i+1}^*\right) \qquad \text{for } i < n$$

$$\varepsilon_i^* = \frac{L}{L^2 + H^2}\left(u_i^*\right) \qquad \text{for } i = n \qquad (4.4)$$

The current stress in the braces of story i is given in Equation 4.5.

$$\sigma_i^* = \min\left(\max\left(\sigma_i^{prev} + E(\varepsilon_i^* - \varepsilon_i^{prev}), -\sigma_y\right), \sigma_y\right) \tag{4.5}$$

where E is Young's modulus of elasticity, σ_y is the yield stress, and σ_i^{prev} and ε_i^{prev} are the previously computed stress and strain in story i, respectively. If $\sigma_i^* = \pm\sigma_y$, then the braces in story i have yielded.

4.1.2 Stiffness Matrix

If the braces in story i have yielded, the current story stiffness is zero, otherwise, the current story stiffness is equal to the elastic stiffness as given in Equation 4.6.

$$\begin{aligned} k_i^* &= 0 && \text{if } \sigma_i^* = \pm\sigma_y \\ k_i^* &= \frac{EA_iL^2}{\left(L^2 + H^2\right)^{3/2}} && \text{otherwise} \end{aligned} \tag{4.6}$$

If there are 5 stories in the frame, then the current stiffness matrix is given in Equation 4.7.

$$\mathbf{K}^* = \begin{bmatrix} k_1^* & -k_1^* & 0 & 0 & 0 \\ -k_1^* & k_1^* + k_2^* & -k_2^* & 0 & 0 \\ 0 & -k_2^* & k_2^* + k_3^* & -k_3^* & 0 \\ 0 & 0 & -k_3^* & k_3^* + k_4^* & -k_4^* \\ 0 & 0 & 0 & -k_4^* & k_4^* + k_5^* \end{bmatrix} \tag{4.7}$$

4.1.3 Resistance Vector

The current horizontal resistance force provided by the braces in story i is given in Equation 4.8.

$$r_i^* = \frac{LA_i\sigma_i^*}{\sqrt{L^2 + H^2}} \tag{4.8}$$

If there are five stories, the current resistance vector is given in Equation 4.9.

$$\mathbf{R}^* = \begin{Bmatrix} r_1^* \\ r_2^* - r_1^* \\ r_3^* - r_2^* \\ r_4^* - r_3^* \\ r_5^* - r_4^* \end{Bmatrix} \tag{4.9}$$

4.1.4 Force Vector

For a building subject to horizontal ground acceleration, $\ddot{u}_g$, the effective horizontal force is the same at every story. If there are five stories, the force vector is given in Equation 4.10.

$$\mathbf{F} = -m\ddot{u}_g \begin{Bmatrix} 1 \\ 1 \\ 1 \\ 1 \\ 1 \end{Bmatrix} = -m\ddot{u}_g \mathbf{1} \tag{4.10}$$

where **1** is a vector of one's.

4.1.5 Mass Matrix

It is assumed that the mass is constant with time and is the same for all stories. Let the mass at each story be m. If there are five stories, then the mass matrix is given in Equation 4.11.

$$\mathbf{M} = m \begin{bmatrix} 1 & 0 & 0 & 0 & 0 \\ 0 & 1 & 0 & 0 & 0 \\ 0 & 0 & 1 & 0 & 0 \\ 0 & 0 & 0 & 1 & 0 \\ 0 & 0 & 0 & 0 & 1 \end{bmatrix} = m\mathbf{I} \tag{4.11}$$

where **I** is the identity matrix.

4.1.6 Damping Matrix

It is assumed that the damping matrix is constant with time and is mass-proportional. Let the damping ratio be ζ, and let the natural circular frequency of the fundamental elastic mode be ω. If there are five stories, then the damping matrix is given in Equation 4.12.

$$\mathbf{C} = 2m\zeta\omega\begin{bmatrix} 1 & 0 & 0 & 0 & 0 \\ 0 & 1 & 0 & 0 & 0 \\ 0 & 0 & 1 & 0 & 0 \\ 0 & 0 & 0 & 1 & 0 \\ 0 & 0 & 0 & 0 & 1 \end{bmatrix} = 2m\zeta\omega\,\mathbf{I} \tag{4.12}$$

The damping ratio is specified by the user, and ω for the fundamental elastic mode is determined by inverse vector iteration which begins with a starting vector of one's, $\mathbf{v}_0 = \mathbf{1}$, and iterates as shown in Equation 4.13.

$$\mathbf{v}_{k+1} = \mathbf{K}^{-1}\mathbf{M}\mathbf{v}_k = m\mathbf{K}^{-1}\mathbf{v}_k \tag{4.13}$$

where the vector $\mathbf{v}^{k+1}$ becomes the mode shape vector for the fundamental mode and $\mathbf{K}$ is the elastic stiffness matrix (no plastic yielding).

At each iteration, the natural circular frequency is calculated from the Rayleigh quotient as shown in Equation 4.14.

$$\omega = \sqrt{\frac{\mathbf{v}_k^T \mathbf{K} \mathbf{v}_k}{\mathbf{v}_k^T \mathbf{M} \mathbf{v}_k}} = \sqrt{\frac{\mathbf{v}_k^T \mathbf{K} \mathbf{v}_k}{m \mathbf{v}_k^T \mathbf{v}_k}} \tag{4.14}$$

where iteration stops when the change in ω is negligible.

4.2 Nonlinear Response History Analysis

Newmark's average acceleration procedure with Newton-Raphson iteration is used to integrate Equation (4.1) which is a second-order nonlinear differential equation. Average acceleration has been proven to be a stable integration technique equivalent to the trapezoidal rule (Chopra, 1995). The ground acceleration, $\ddot{u}_g$, changes with time. It is normally specified as a set of discrete values at equally spaced time steps ranging from one to nstep. This set of discrete values is called an accelerogram. Let $\ddot{u}_g^j$ be the ground acceleration at the jth time step, and let Δt be the length of time between time steps.

Average acceleration assumes that the acceleration throughout each time step is constant. Thus, the acceleration at all times between time step j and time step j+1 is given in Equation 4.15.

$$\ddot{\mathbf{U}} = \frac{1}{2}\left(\ddot{\mathbf{U}}^j + \ddot{\mathbf{U}}^{j+1}\right) \tag{4.15}$$

Acceleration is then integrated to get velocity given by Equation 4.16.

$$\dot{\mathbf{U}} = \frac{t}{2}\left(\ddot{\mathbf{U}}^{j} + \ddot{\mathbf{U}}^{j+1}\right) + \dot{\mathbf{U}}^{j} \tag{4.16}$$

where the constant of integration is determined such that at t = 0, the velocity is equal to the velocity at time step j.

Now we can integrate velocity to get displacement given in Equation 4.17.

$$\mathbf{U} = \frac{t^2}{4}\left(\ddot{\mathbf{U}}^{j} + \ddot{\mathbf{U}}^{j+1}\right) + t\dot{\mathbf{U}}^{j} + \mathbf{U}^{j} \tag{4.17}$$

where the constant of integration is determined such that at t = 0, the displacement is equal to the displacement at time step j. Evaluating the previous two equations at $t = \Delta t$ is shown in Equations 4.18 and 4.19.

$$\dot{\mathbf{U}}^{j+1} = \frac{\Delta t}{2}\left(\ddot{\mathbf{U}}^{j} + \ddot{\mathbf{U}}^{j+1}\right) + \dot{\mathbf{U}}^{j} \tag{4.18}$$

$$\mathbf{U}^{j+1} = \frac{\Delta t^2}{4}\left(\ddot{\mathbf{U}}^{j} + \ddot{\mathbf{U}}^{j+1}\right) + \Delta t\dot{\mathbf{U}}^{j} + \mathbf{U}^{j} \tag{4.19}$$

Using algebra in the above two equations gives Equations 4.20 and 4.21.

$$\ddot{\mathbf{U}}^{j+1} = \frac{4}{\Delta t^2}\left(\mathbf{U}^{j+1} - \mathbf{U}^{j}\right) - \frac{4}{\Delta t}\dot{\mathbf{U}}^{j} - \ddot{\mathbf{U}}^{j} \tag{4.20}$$

$$\dot{\mathbf{U}}^{j+1} = \frac{2}{\Delta t}\left(\mathbf{U}^{j+1} - \mathbf{U}^{j}\right) - \dot{\mathbf{U}}^{j} \tag{4.21}$$

These are the basic equations used by the Newmark's method to update velocities and accelerations to from time step j to time step j+1.

Writing Equations 4.1, 4.2, and 4.3 at time step j+1 are shown in Equations 4.22, 4.23, and 4.24.

$$\mathbf{M}\ddot{\mathbf{U}}^{j+1} + \mathbf{C}\dot{\mathbf{U}}^{j+1} + \mathbf{R}^{j+1} = \mathbf{F}^{j+1} \tag{4.22}$$

$$\mathbf{R}^{j+1} \approx \mathbf{R}^{*} + \mathbf{K}^{*}\Delta\mathbf{U} \tag{4.23}$$

$$\mathbf{U}^{j+1} = \mathbf{U}^{*} + \Delta\mathbf{U} \tag{4.24}$$

Substituting Equations 4.20, 4.21, 4.23, and 4.24 into Equation 4.22 gives Equation 4.25.

$$\begin{aligned}
&\mathbf{M}\left(\frac{4}{\Delta t^2}\left(\mathbf{U}^{*} + \Delta\mathbf{U} - \mathbf{U}^{j}\right) - \frac{4}{\Delta t}\dot{\mathbf{U}}^{j} - \ddot{\mathbf{U}}^{j}\right) \\
&+ \mathbf{C}\left(\frac{2}{\Delta t}\left(\mathbf{U}^{*} + \Delta\mathbf{U} - \mathbf{U}^{j}\right) - \dot{\mathbf{U}}^{j}\right) \\
&\quad + \mathbf{R}^{*} + \mathbf{K}^{*}\Delta\mathbf{U} = \mathbf{F}^{j+1}
\end{aligned} \tag{4.25}$$

Rearranging Equation 4.25 gives Equation 4.26.

$$\mathbf{K}_D \Delta \mathbf{U} = \mathbf{F}_D \tag{4.26}$$

where:

$$\mathbf{K}_D = \frac{4}{\Delta t^2}\mathbf{M} + \frac{2}{\Delta t}\mathbf{C} + \mathbf{K}^* \tag{4.27}$$

$$\mathbf{F}_D = \mathbf{F}^{j+1} - \mathbf{M}\left(\frac{4}{\Delta t^2}\left(\mathbf{U}^* - \mathbf{U}^j\right) - \frac{4}{\Delta t}\dot{\mathbf{U}}^j - \ddot{\mathbf{U}}^j\right) - \mathbf{C}\left(\frac{2}{\Delta t}\left(\mathbf{U}^* - \mathbf{U}^j\right) - \dot{\mathbf{U}}^j\right) - \mathbf{R}^* \tag{4.28}$$

Substituting Equations 4.10, 4.11, and 4.12 into Equations 4.27 and 4.28 gives Equations 4.29 and 4.30.

$$\mathbf{K}_D = m\left(\frac{4}{\Delta t^2} + \frac{4\zeta\omega}{\Delta t}\right)\mathbf{I} + \mathbf{K}^* \tag{4.29}$$

$$\mathbf{F}_D = -m\left(\ddot{u}_g^{j+1}\mathbf{1} + \left(\frac{4}{\Delta t^2} + \frac{4\zeta\omega}{\Delta t}\right)\left(\mathbf{U}^* - \mathbf{U}^j\right) - \left(\frac{4}{\Delta t} + 2\zeta\omega\right)\dot{\mathbf{U}}^j - \ddot{\mathbf{U}}^j\right) - \mathbf{R}^* \tag{4.30}$$

The nonlinear response history analysis procedure is summarized as follows:

1) Initialize $\mathbf{U}^j = \dot{\mathbf{U}}^j = \ddot{\mathbf{U}}^j = \mathbf{U}^* = \mathbf{0}$ and $\sigma_i^{prev} = \varepsilon_i^{prev} = \varepsilon_i^{max} = 0$ for i = 1 to n

2) Loop j = 1 to ntime

3) Loop until mag < user-specified tolerance

4) Calculate current strains at each story by Equation 4.4

5) Calculate current stresses at each story by Equation 4.5

6) Calculate the current stiffness matrix by Equations 4.6-4.7

7) Calculate the current resistance vector by Equations 4.8-4.9

8) Calculate the dynamic stiffness matrix by Equation 4.29

9) Calculate the dynamic force vector by Equation 4.30

10) Solve Equation 4.26 for $\Delta\mathbf{U}$

11) Update the current displacements $\mathbf{U}^* = \mathbf{U}^* + \Delta\mathbf{U}$

12) Calculate mag = Euclidean length of vector $\Delta\mathbf{U}$

13) Update $\mathbf{U}^{j+1} = \mathbf{U}^*$

14) Update $\dot{\mathbf{U}}^{j+1}$ by Equation 4.21

15) Update $\ddot{\mathbf{U}}^{j+1}$ by Equation 4.20

16) Update $\sigma_i^{prev} = \sigma_i^*$, $\varepsilon_i^{prev} = \varepsilon_i^*$, $\varepsilon_i^{max} = \max(\varepsilon_i^{max}, |\varepsilon_i^*|)$ for i = 1 to n

The above procedure is performed for each of multiple ground accelerogram records.

4.3 Optimization

Design of the BRB's in a braced frame can be cast as the following optimization problem:

Find: A_i i = 1 to n

Minimize: $\sum_{i=1}^{n} A_i$

Satisfy: $\frac{E}{\sigma_y}\varepsilon^{ave\,max} \le$ allowable ductility factor

Satisfy: $$\frac{L^2 + H^2}{LH}\varepsilon^{ave\,max} \leq \text{allowable inter-story drift}$$

Where: $$\varepsilon^{ave\,max} = \frac{\sum_{k=records}\left(\max_{i=stories}\left(\varepsilon_{ik}^{max}\right)\right)}{nrecord}$$

The design variables are the cross-sectional areas of the BRB's for each story. The objective is to minimize the sum of these cross-sectional areas. There are two constraints. The first is on ductility and the second is on inter-story drift. Both constraints are functions of ε^{avemax}. The dynamic nonlinear analysis calculates ε_{ik}^{max}, which is the maximum strain over the time steps for story i and accelerogram record k. Therefore, ε^{avemax} is the maximum strain over time steps and stories, averaged over the records. This is in accordance with 2003 Edition of FEMA 450 which allows maximum response to be averaged over records if there are seven or more records. If there are fewer than seven records, the maximum strain rather than the average strain shall be used.

A genetic algorithm is used to solve the above optimization problem. This algorithm has the following five parameters:

ngener = number of generations

nsize = generation size

ntourn = selection tournament size

probcross = crossover probability

probmutate = mutation probability

Input to the genetic algorithm consists of values for the above five algorithm parameters as well as the minimum and maximum values for each design variable. Output from the algorithm consists of the optimum value of each design variable. As stated above, the design variables for this research project are the BRB cross-sectional areas for each story. The steps of the genetic algorithm are:

1) Loop i = 1 to ngener

2) If i = 1, randomly generate parent generation consisting of nsize chromosomes

3) If i > 1, generate children from parents via selection/crossover/mutation

4) Analyze any new chromosomes and get fitness of each

5) If i > 1, next parent generation = nsize most fit parent or child chromosomes

The genetic algorithm loops through generations with each generation consisting of nsize chromosomes. A chromosome is a representation of a design. If there are ndv design variables, then each chromosome has ndv genes, and each gene is a real-valued number equal to the value of the corresponding design variable. If one is optimizing the design of a five-story building with BRB's. Then all of the chromosomes have five genes, and the value of the jth gene is the cross-sectional area of the BRB's in the jth story. Different chromosomes have different values for the cross-sectional areas, and thus, each chromosome represents a different design. The genetic algorithm searches for the optimum chromosome.

In step 2 of the genetic algorithm a starting generation of chromosomes is randomly created. This is accomplished by randomly generating values for each of the

ndv genes in each of the nsize chromosomes. The random values must be between the specified minimum and maximum values for each gene (design variable).

Steps 3 and 5 of the genetic algorithm are skipped for the first generation (i = 1). In step 4, the new chromosomes in the parent generation are analyzed which requires calculating the objective and constraints for each chromosome. In this research, the objective is the sum of the cross-sectional areas, or in other words, the sum of the values of the genes in the chromosome. The objective is a positive number, and we desire to minimize it. There are two constraints, one on ductility and one on inter-story drift. Nonlinear dynamic analysis is performed for each of the accelerogram records using the cross-sectional areas given by the gene values of the chromosome. The average maximum strain ε^{avemax} is calculated for the chromosome. Both constraints are then evaluated to compute the feasibility of the chromosome as shown in Equation 4.31.

$$\text{feasibility} = \max\left(1, \frac{E\varepsilon^{\text{ave max}}}{\sigma_y \text{ductility}}, \frac{(L^2 + H^2)\varepsilon^{\text{ave max}}}{(LH)\text{drift}}\right) - 1 \qquad (4.31)$$

where, ductility = allowable ductility factor, and drift = allowable inter-story drift.

If both constraints are satisfied, the feasibility will equal zero, meaning the chromosome is feasible. If either constraint is violated, the feasibility will be greater than zero, and equal to the maximum constraint violation, meaning the chromosome is infeasible.

After calculating the value of the objective and the feasibility for a chromosome, its fitness is determined. The fitness is a single number representing the quality of the

chromosome. The higher the fitness, the better the design represented by the chromosome. For all feasible chromosomes (feasibility = 0) fitness is calculated in Equation 4.32.

$$\text{fitness} = 1/\text{objective} \tag{4.32}$$

where, minimizing the objective maximizes the fitness.

For all infeasible chromosomes (feasibility > 0) fitness is calculated in Equation 4.33.

$$\text{fitness} = 1/(\text{maxobj}+\text{feasibility}) \tag{4.33}$$

where maxobj is the maximum objective value for all feasible chromosomes in the generation. This insures that the fitness of all infeasible chromosomes in the generation is lower than the worst feasible chromosome.

In step 3 of the genetic algorithm, nsize children chromosomes are generated two at a time from the previous parent generation. Three sub-steps are executed to generate two children, namely selection, crossover, and mutation.

In the selection substep, a father chromosome is selected from the previous parent generation by a simple process known as tournament selection. One of the algorithm parameters is ntourn = tournament size, which is much less than the generation size. The ntourn chromosomes are randomly selected from of the parent generation, and the one with the highest fitness is the father chromosome. The same process is used to select a

mother chromosome from the parent generation. It is a remote possibility that the father and mother chromosomes are the same.

In the crossover substep, two children chromosomes are generated by mating the father and mother chromosomes. A random number between zero and one is generated. If this number is less than the algorithm parameter probcross, crossover is executed. Otherwise, the father chromosome is copied as the first child chromosome, and the mother chromosome is copied as the second child chromosome. If crossover is to be executed, it is done gene by gene. A random number r is generated for each gene. Let x_1 be the father value and x_2 be the mother value for the particular gene. The gene values y_1 and y_2 for the two children are calculated in Equations 4.34 and 4.35.

$$y_1 = rx_1 + (1 - r)x_2 \tag{4.34}$$

$$y_2 = rx_2 + (1 - r)x_1 \tag{4.35}$$

This form of crossover is known as blend crossover and it insures that the gene values for the children are between the gene values of the father and mother.

In the mutation substep, a few of the genes of the children chromosomes are randomly changed to new values. First, loop through each of the genes of the two children chromosomes. For each gene, generate a random number between zero and one. If this number is less than the algorithm parameter probmutate, the gene is mutated. Otherwise, the gene is left alone. The parameter probmutate is typically a low value such as 0.01 or 0.001. Thus, mutation is executed on rare occasion. Suppose the current value of the gene to be mutated is x. Suppose the minimum and maximum values for this gene

are x_{min} and x_{max}, respectively. A random number is generated between x_{min} and x_{max}. The new gene value is calculated as in Equations 4.36 and 4.37.

$$y = x_{min} + (r - x_{min})^{\alpha}(x - x_{min})^{1-\alpha} \qquad \text{if } r \le x \tag{4.36}$$

$$y = x_{max} - (x_{max} - r)^{\alpha}(x_{max} - x)^{1-\alpha} \qquad \text{if } r > x \tag{4.37}$$

The value of the parameter α is calculated as by Equation 4.38.

$$\alpha = \frac{\text{ngener} - i + 1}{\text{ngener}} \tag{4.38}$$

where for the first generation (i=1), the parameter $\alpha = 1$, which makes $y = r$. This case is known as uniform mutation meaning the mutated value is any value between x_{min} and x_{max} with equal probability. If ngener is a large number, then for the final generation (i=ngener), the parameter $\alpha \approx 0$, which makes $y = x$, meaning that the gene is not mutated at all. As generations increase from one to ngener, α decreases in value from one to zero, and the probability that y is closer to x increases. Thus, in the starting generations, mutations can be quite large, while in the final generations, mutations are small.

The success of a genetic algorithm depends on three characteristics: fitness pressure, inheritance, and diversity. The selection substep exercises fitness pressure by selecting parents according to their fitness. The crossover substep insures that children

inherit values similar to those of their parents. The mutation substep allows diversity to enter into the genetic algorithm.

Step 5 of the genetic algorithm is often referred to as elitism. It basically says that after generating children chromosomes in step 3 and calculating their fitnesses in step 4, the children must compete with their parents for survival. The nsize chromosomes with the highest fitnesses among the nsize parent chromosomes and the nsize children chromosomes become the parent chromosomes for the next generation. This step insures that the best chromosomes survive from generation to generation.

The genetic algorithm does not require the calculation of gradients that are required by calculus-based algorithms. In fact, the constraints in this research project involve max functions which are not differentiable. The genetic algorithm is more efficient than brute-force methods such as exhaustive search and random search. The genetic algorithm is also very easy to implement. These are the reasons for choosing the genetic algorithm as the optimization algorithm.

5 Consistent Input and Output Parameters

In this chapter the input and output parameters for both procedures are discussed. Where parameters are different between the two procedures, consistency must be maintained to make an accurate comparison of the two procedures. Input parameters that are needed for both procedures are:

n = number of stories

H = story height (same for all stories)

L = bay width (same for all bays)

m = story mass (same for all stories)

ζ = damping ratio = 5% (typical for BRBF's)

E = Young's modulus of elasticity = 29000 ksi

Additional input parameters for the Equivalent Lateral Force procedure are:

Location of the site needed to access USGS seismicity maps

Soil type = Site Class D

I = importance factor = 1.0

F_y = yield stress for steel BRB's = 45 ksi

Additional input parameters for the Optimized Response History procedure are:

ngener = number of generations = 50

nsize = generation size = 50

ntourn = tournament size = 6

probcross = crossover probability = 0.6

probmutate = mutation probability = 0.1

minimum cross-sectional area

maximum cross-sectional area

allowable ductility ratio

allowable drift

σ_y = yield stress

nrecords = number of accelerogram records = 10

Δt = time step = 0.005 s

tol = Newton-Raphson convergence tolerance = 10^{-7} in

ntime for each accelerogram record = number of time steps

scale factor for each accelerogram record

accelerogram record values in percent g

Output parameters for both procedures are:

A_i for each story i = 1 to n

5.1 Mass Independence

In the NTHO procedure, the mass matrix, damping matrix, and force vector are proportional to the mass of the structure m. This suggests that the equation of motion (Equation 4.1) can be divided by m. Dividing the stiffness matrix by m is equivalent to dividing the cross-sectional areas by m. Therefore, m need not be an input parameter, rather the output cross-sectional areas are actually cross-sectional areas divided by m.

In the ELF procedure, the base shear is also proportional to m (see Equation 3.6). The story forces, axial forces, and drifts are also proportional to m. Therefore, m need not be an input parameter and the output cross-sectional areas are actually divided by m.

5.2 Variable Input Parameters

The input parameters n, H, L, and site location were varied in this study. The number of stories (n) considered were 1, 3, and 5 stories. The story heights (H) considered were 10ft, 12ft, 14ft, and 16ft. The bay widths (L) considered were 10ft, 15ft, 20ft, 25ft, 30ft, and 35ft. Three different locations were considered representing sites with high, medium, and low seismicity.

The genetic algorithm parameters minimum area/m and maximum area/m were varied from execution to execution. On the initial execution, a broad range was assumed. For example, the minimum area/m = 0.5 $in^3/kip/s^2$ and maximum area/m = 10 $in^3/kip/s^2$. On the second execution, the maximum and minimum area/m were reset to plus and minus 1 $in^3/kip/s^2$ from the optimum values output from the first execution for each story. In similar fashion, successive executions were made with tighter and tighter ranges. If, at any point, an optimum value was significantly close to the minimum value or the maximum value, these values were relaxed in the next execution.

5.3 Consistent Accelerogram Scale Factors

Ten different accelerograms were selected for the Optimized Response History Method. These accelerograms are shown in Figure 5-1 through 5-10.

The accelerograms were scaled to represent the design level ground motions for a particular site. The scaling was consistent with the philosophy used in the ELF procedure. The determination of the scaling factor for each accelerogram involves three steps.

First, a pseudo-acceleration response spectrum, S_{psa}, is developed for each accelerogram representing the maximum linear dynamic response of a single degree-of-freedom system as a function of period. The pseudo-acceleration response spectra corresponding to the ten accelerograms are shown in Figures 5-11 through 5-20.

Second, a design response spectrum is generated for a particular site. The design response spectrum is constructed in the same fashion as outlined in the ELF procedure (see Section 3.1). The three design response spectra corresponding to the three sites (high, medium, and low seismicity) are plotted on Figure 5-11 through 5-20.

Third, the scale factor for each accelerogram is calculated. Both the pseudo-acceleration response spectrum and the design response spectrum are evaluated at several equally-spaced periods between 0.6 seconds and 1.5 seconds representing the range of fundamental periods for one to five story braced frames. The scale factor is calculated using Equation 5.1.

$$\text{scale factor} = \frac{\sum_{0.6}^{1.5} S_a}{\sum_{0.6}^{1.5} S_{psa}} \tag{5.1}$$

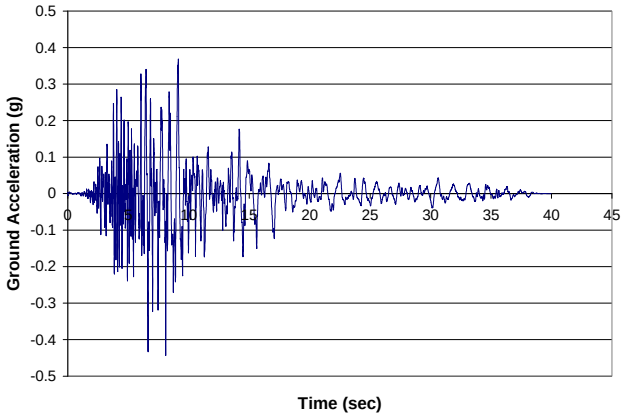

Figure 5-1 Accelerogram 1

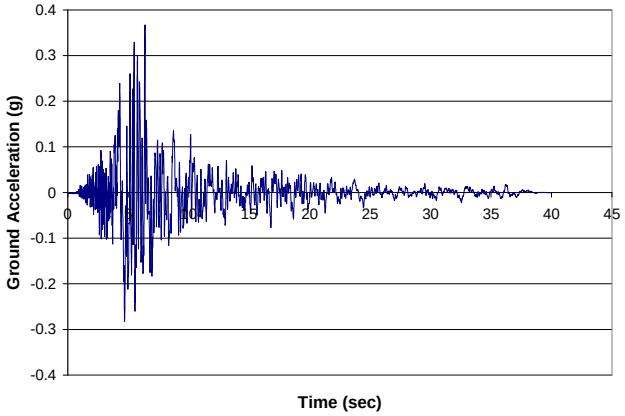

Figure 5-2 Accelerogram 2

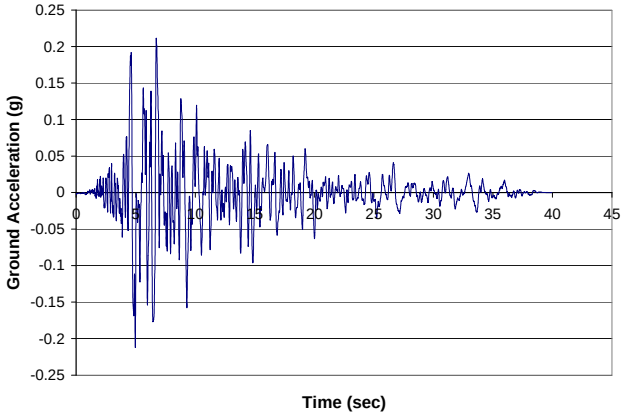

Figure 5-3 Accelerogram 3

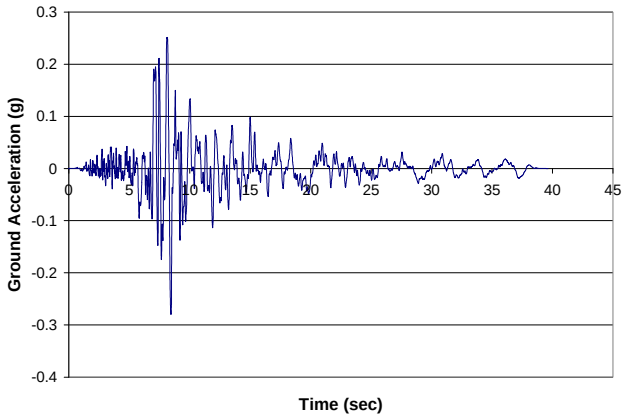

Figure 5-4 Accelerogram 4

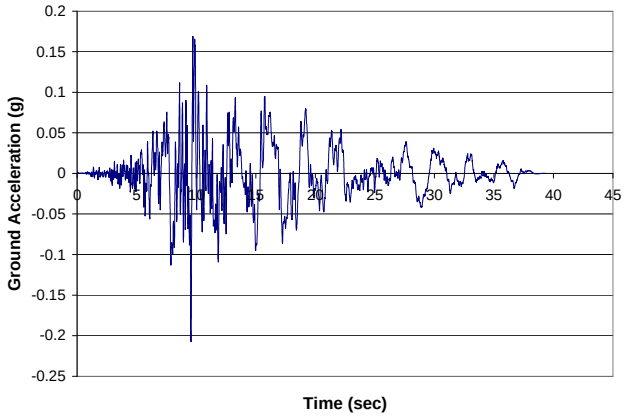

Figure 5-5 Accelerogram 5

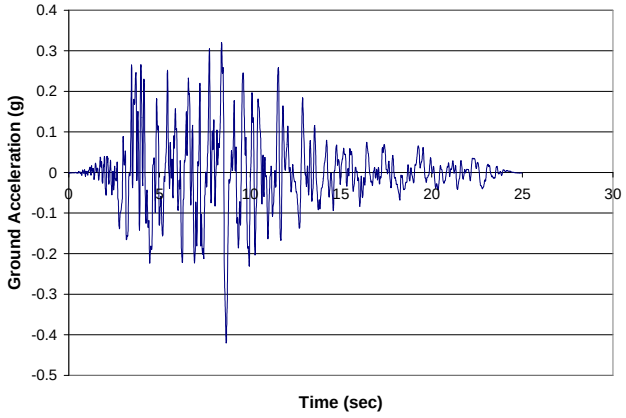

Figure 5-6 Accelerogram 6

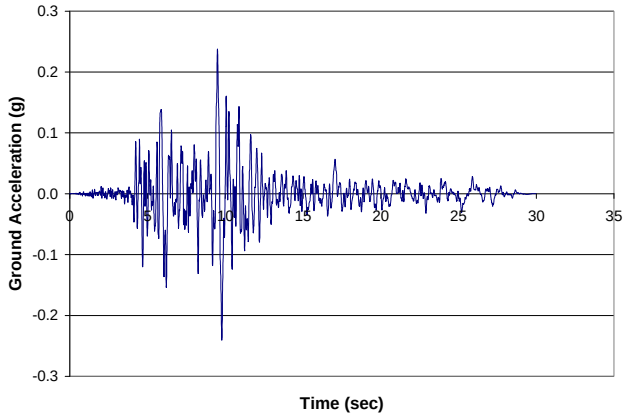

Figure 5-7 Accelerogram 7

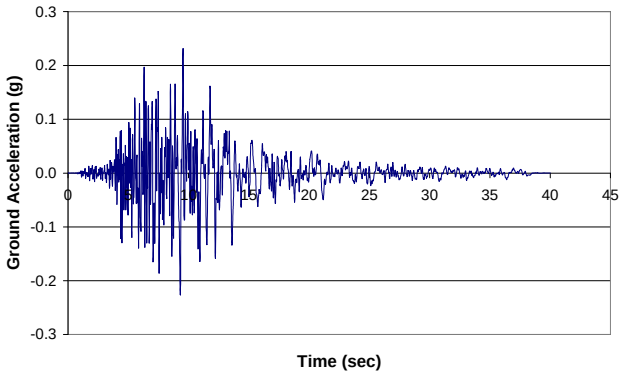

Figure 5-8 Accelerogram 8

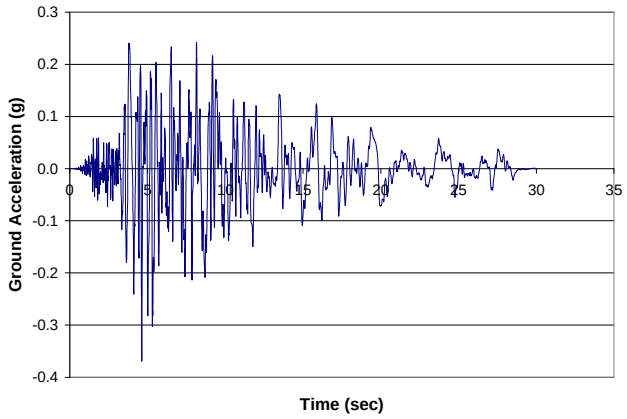

Figure 5-9 Accelerogram 9

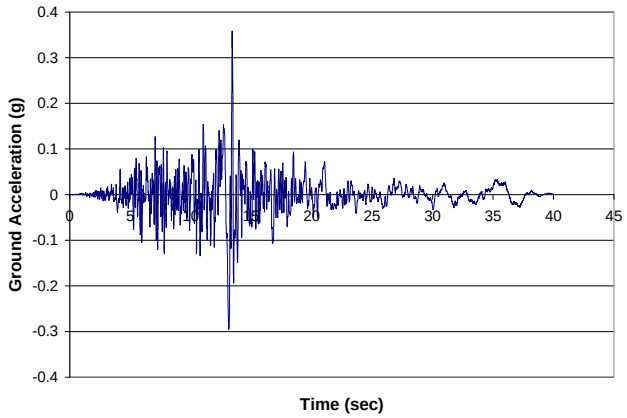

Figure 5-10 Accelerogram 10

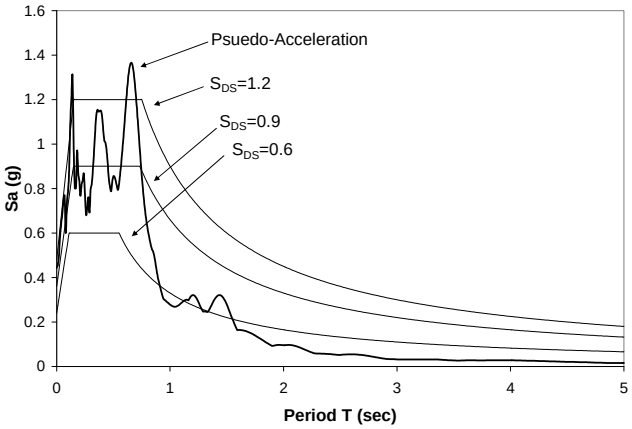

Figure 5-11 Pseudo-Acceleration 1

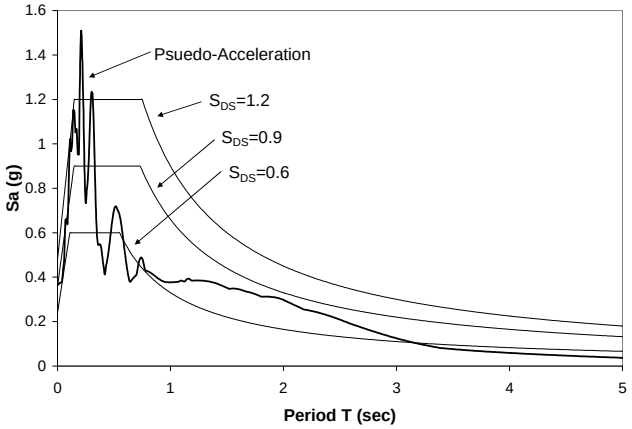

Figure 5-12 Pseudo-Acceleration 2

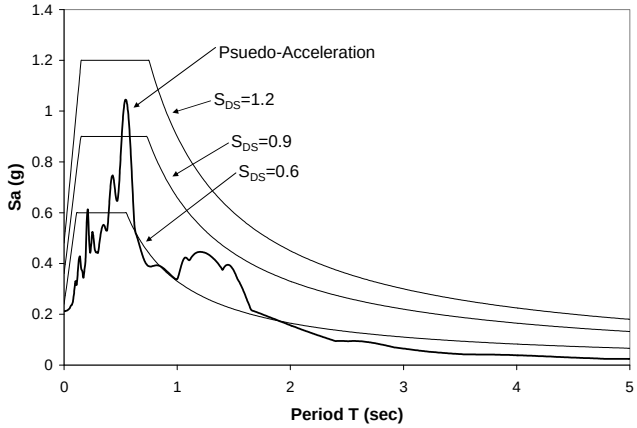

Figure 5-13 Pseudo-Acceleration 3

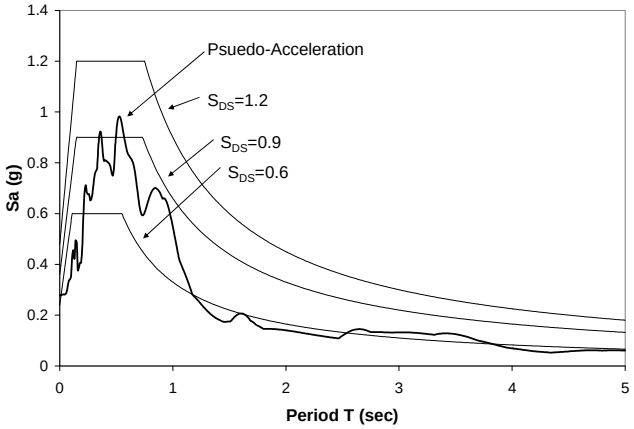

Figure 5-14 Pseudo-Acceleration 4

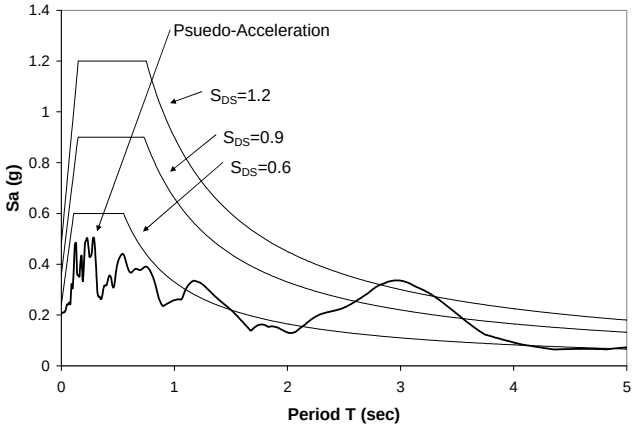

Figure 5-15 Pseudo-Acceleration 5

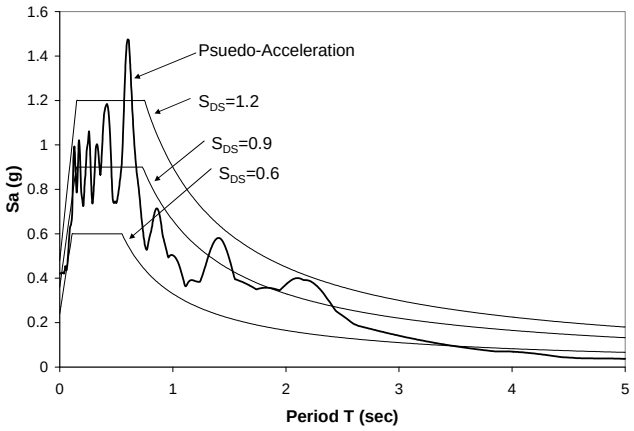

Figure 5-16 Pseudo-Acceleration 6

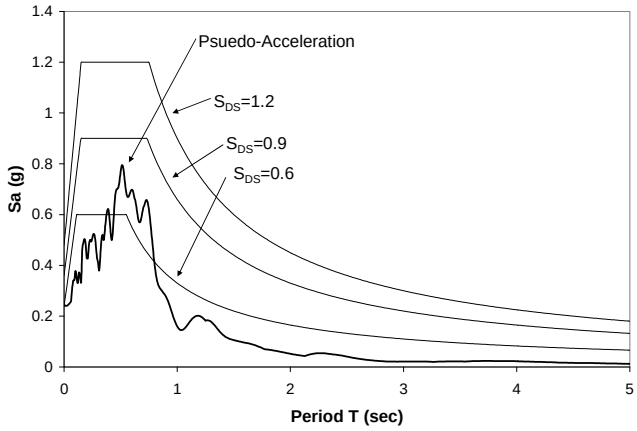

Figure 5-17 Pseudo-Acceleration 7

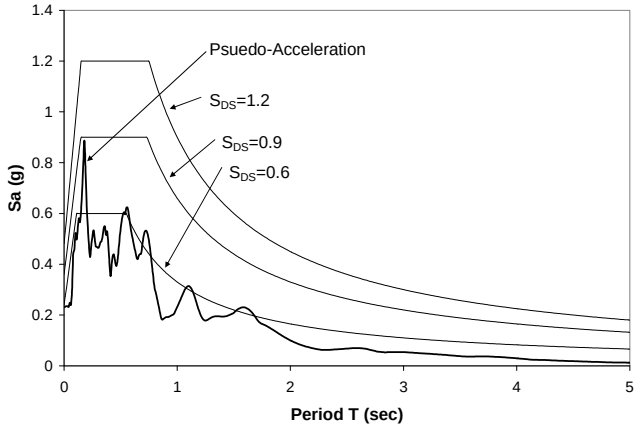

Figure 5-18 Pseudo-Acceleration 8

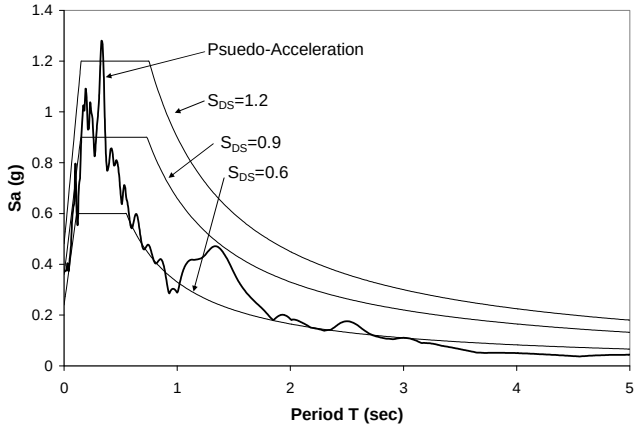

Figure 5-19 Pseudo-Acceleration 9

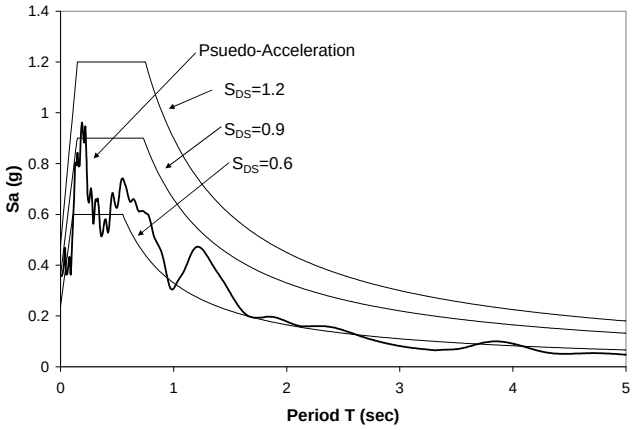

Figure 5-20 Pseudo-Acceleration 10

The scale factors calculated for each pseudo-acceleration are tabulated in Table 5-1.

Table 5-1 Scale Factors

Psuedo-Acceleration	S_{DS}=1.2	S_{DS}=0.9	S_{DS}=0.6
1	1.809	1.333	0.682
2	2.266	1.670	0.854
3	2.158	1.590	0.813
4	1.963	1.446	0.739
5	2.949	2.173	1.111
6	1.511	1.114	0.569
7	3.156	2.326	1.189
8	3.244	2.391	1.222
9	2.111	1.555	0.795
10	1.978	1.457	0.745

5.4 Consistent Allowable Ductility

The allowable ductility in the Optimized Response History Method must be consistent with the assumptions used in the Equivalent Lateral Force Method. The relationship between base shear and lateral displacement for the Equivalent Lateral Force Method is shown in Figure 5-21.

The allowable ductility for BRBF's is calculated using Equation 5.2.

$$\mu = \frac{\Delta_{max}}{\Delta_y} = \frac{V_e}{V_y} = \frac{RV_S}{\Omega_0 V_S} = \frac{R}{\Omega_0} = \frac{7}{2} = 3.5 \qquad (5.2)$$

where R is the response modification coefficient, and Ω_0 is the overstrength coefficient

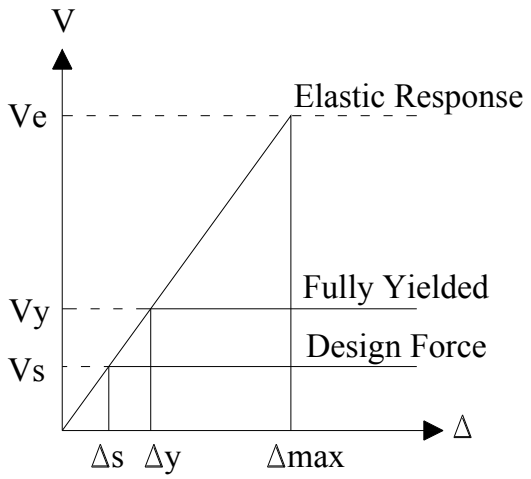

Figure 5-21 Ductility Ratio Diagram (FEMA 450, 2003)

.

5.5 Consistent Allowable Drift

The 2003 edition of FEMA 450 permits the Optimized Response History Method to use 125% of the allowable drift used in the Equivalent Lateral Force Method as described in Section 2.6. Thus, the allowable drift in the Optimized Response History Method is 0.025H for frames with five or more stories and 0.03125H for frames with four or less stories.

5.6 Consistent Yield Stress

The 2003 edition of FEMA 450 requires that experiments be conducted to obtain the force-deformation behavior of BRB's. Such experiments produced the behavior shown in Figure 5-22.

FEMA 450 states that the model for yield stress must account for overstrength, strain hardening, and hysteretic strength degradation. Accordingly, the yield strength was taken as:

$$\sigma_y = 1.95F_y = 1.95(45\text{ksi}) = 87.75\text{ksi} \tag{5.3}$$

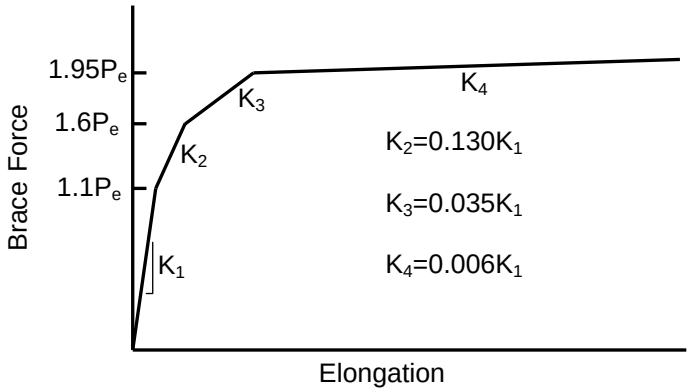

Figure 5-22 BRB Overstrength (Coy, 2007)

5.7 Consistent ϕ Factor

In the Equivalent Lateral Force Method, the $\phi = 0.9$ factor is used in the yield criterion (Equation 3.12). When yielding controls, this factor effectively increases the cross-sectional area (Equation 3.13). The ϕ factor accounts for material and construction variability. To be consistent, it was decided to increase the cross-sectional area in all stories in the Optimized Nonlinear Time History Method in those cases where ductility controls rather than drift.

6 Results

One, three, and five-story BRBF's were designed using the ELF and NTHO procedures with story heights of 10ft, 12ft, 14ft, and 16ft and bay widths of 10ft, 15ft, 20ft, 25ft, 30ft, and 35ft under severe (S_{DS}=1.2), moderate (S_{DS}=0.9), and low (S_{DS}=0.6) seismic loadings. In Section 6.1, graphs that compare results from the two procedures are presented. In Section 6.2, tables indicating which constraints controlled the design for each of the two procedures are shown. In Section 6.3, design charts based on results from the NTHO procedure are displayed.

6.1 Comparison Graphs

The graphs which follow in Figures 6-1 through 6-9 show brace areas divided by mass (A/m) for one-story frames and the sum of the of the brace areas divided by total mass for three and five-story frames (Sum (A/m)). The A/m or sum of A/m is plotted versus the ratio of story height to bay width (H/L). The dashed lines represent the brace A/m determined by the NTHO procedure and the solid lines represent the brace A/m determined by the ELF procedure. Story heights are represented by different data point shapes found in the legend of each graph. In cases where the ELF procedure gives a lower A/m than the NTHO procedure, the ELF procedure is regarded as unconservative

since the NTHO procedure is regarded as a more accurate determination of optimum A/m.

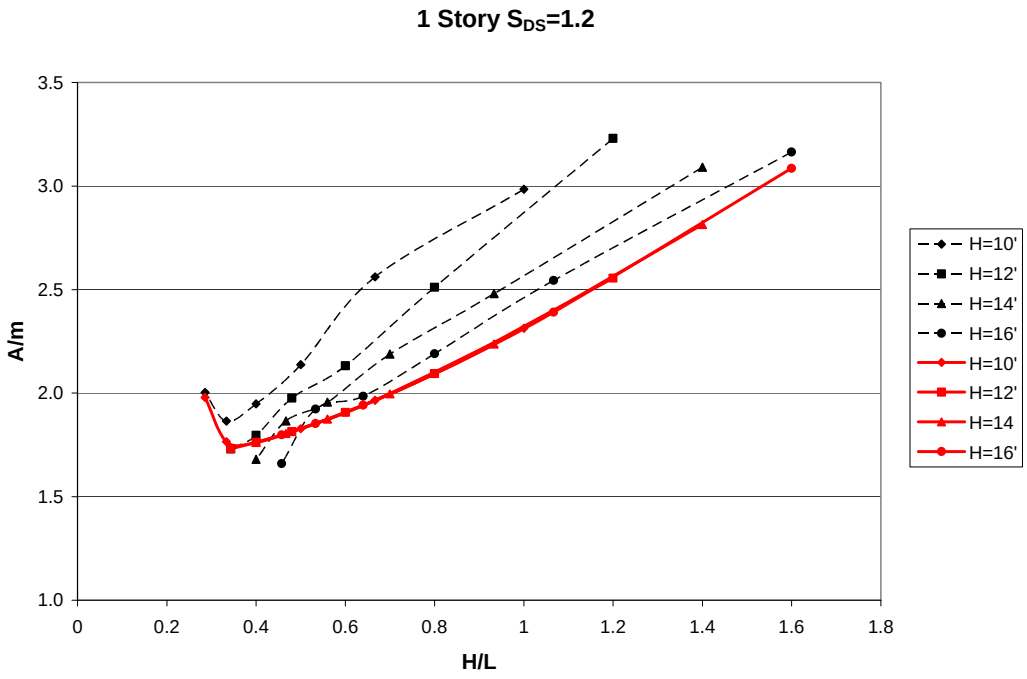

Figure 6-1 One-Story S_{DS}=1.2 A/m

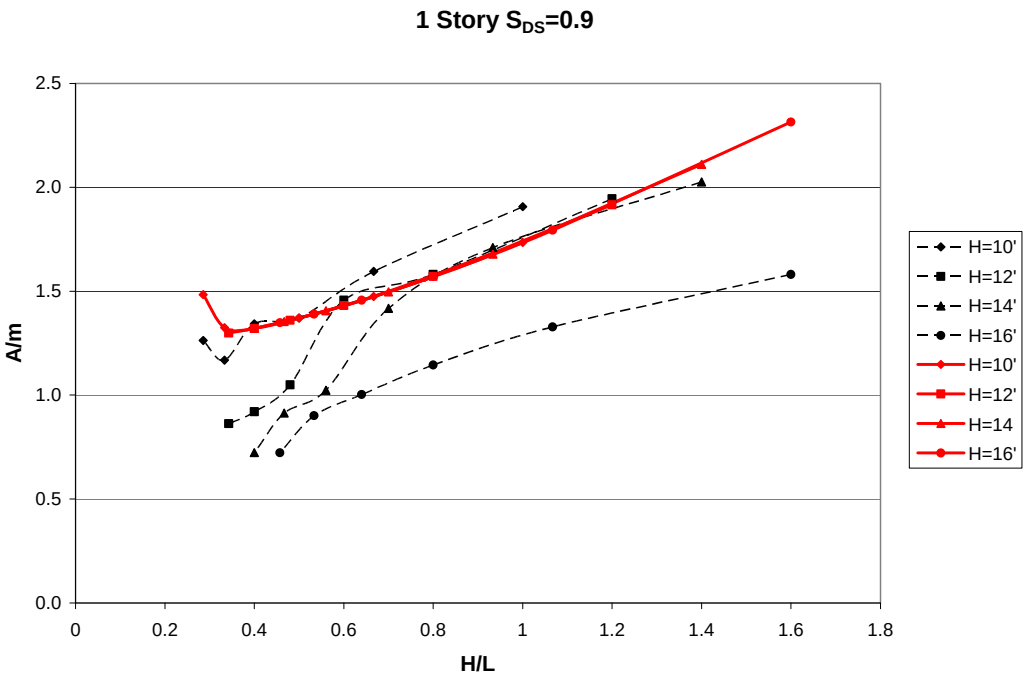

Figure 6-2 One-Story S_{DS}=0.9 A/m

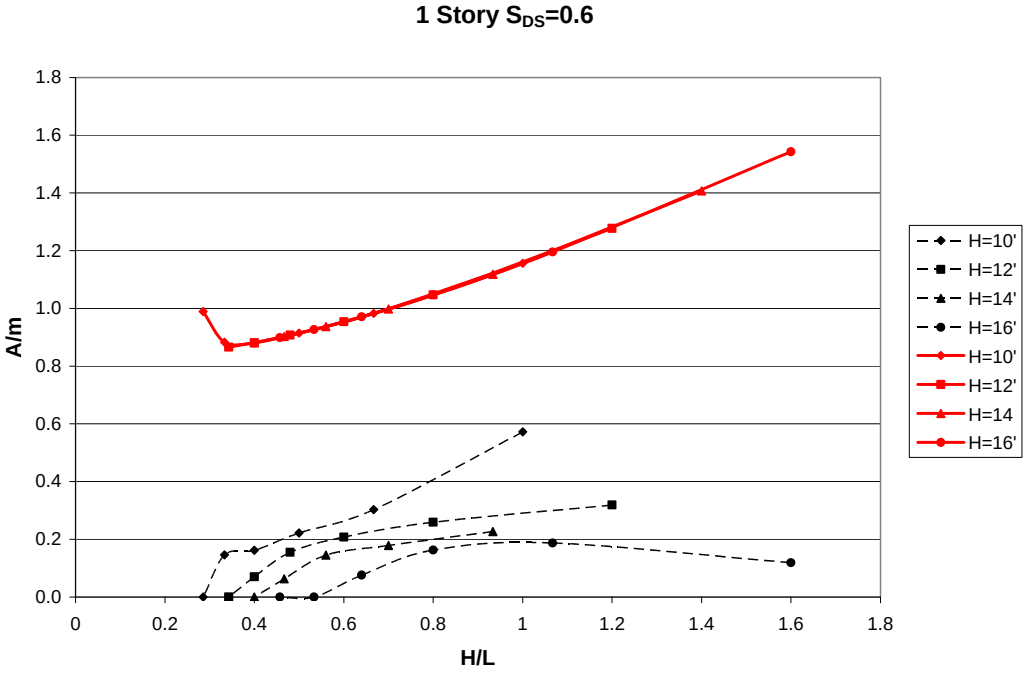

Figure 6-3 One-Story S_{DS}=0.6 A/m

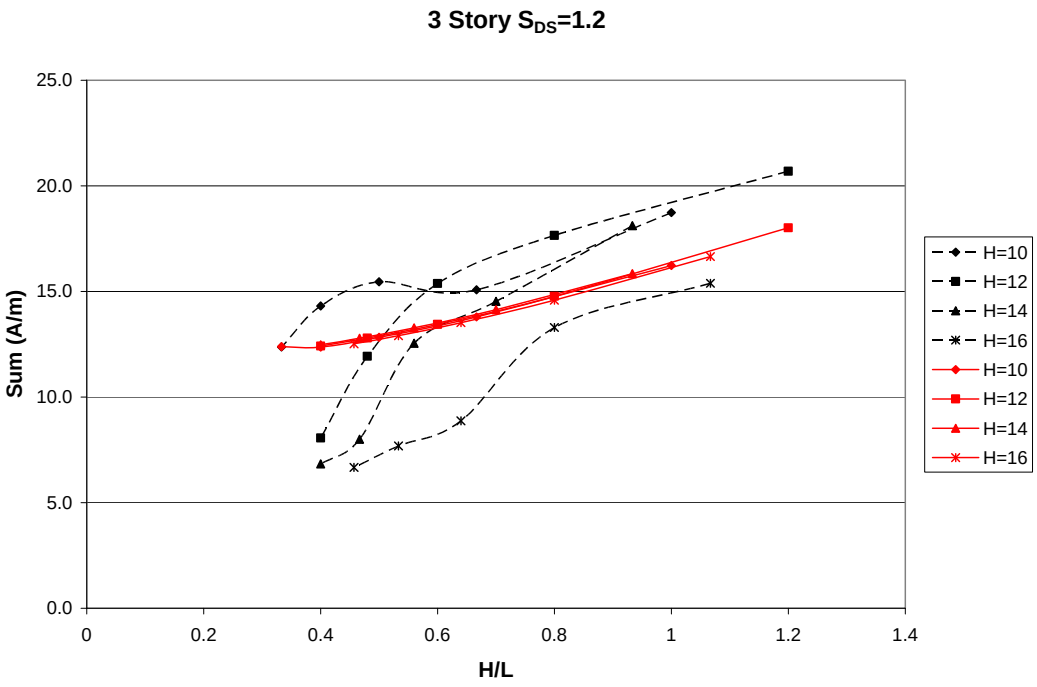

Figure 6-4 Three-Story S_{DS}=1.2 A/m

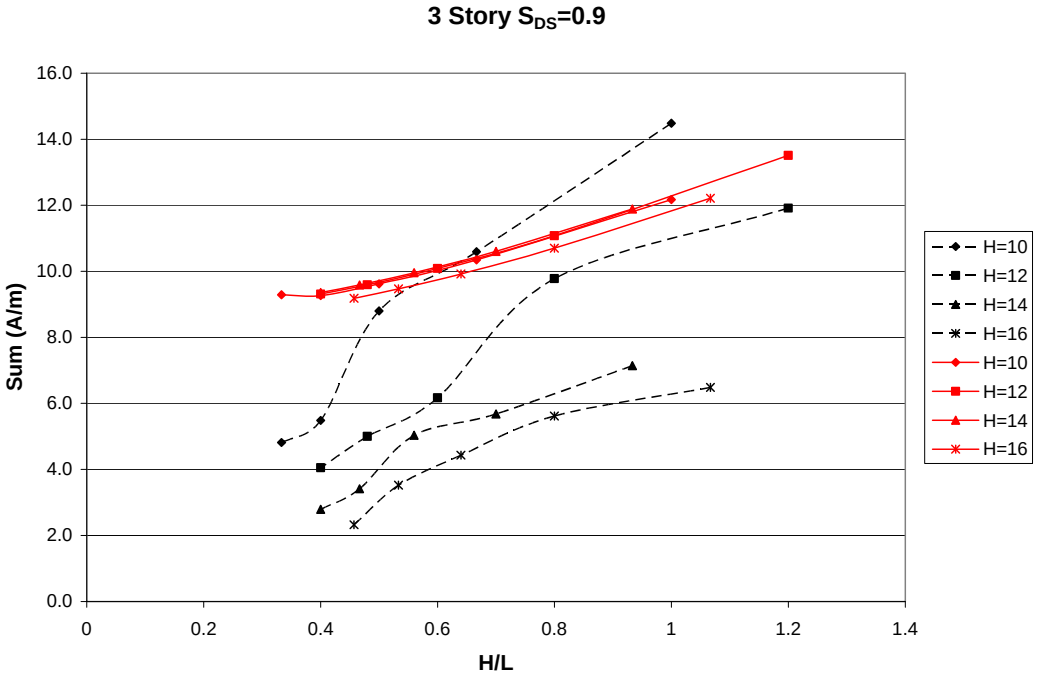

Figure 6-5 Three-Story S_{DS}=0.9 A/m

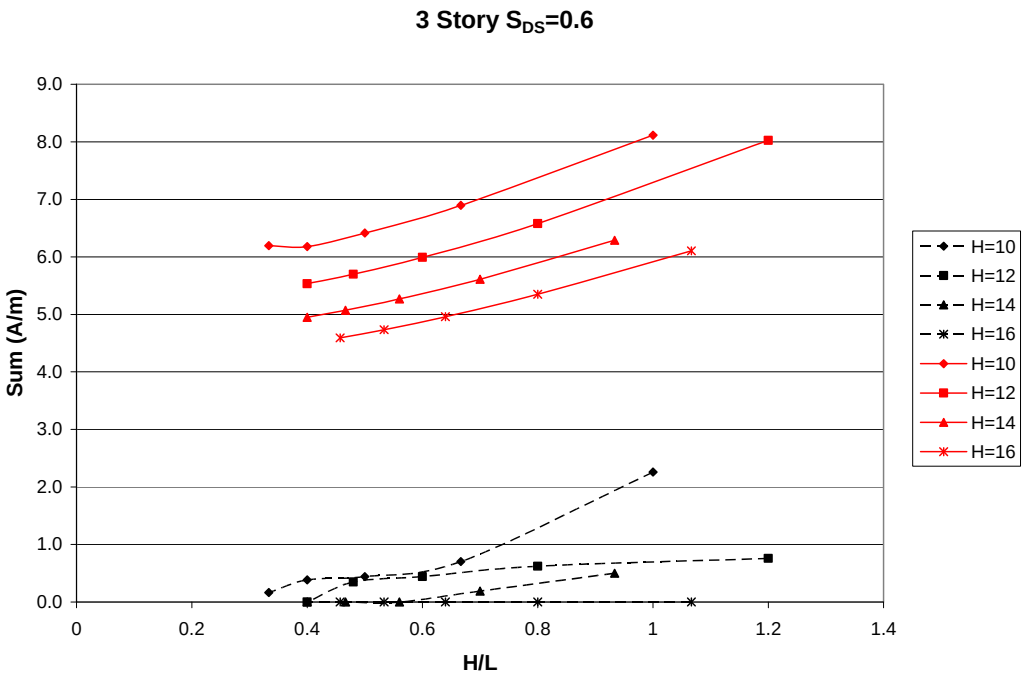

Figure 6-6 Three-Story S_{DS}=0.6 A/m

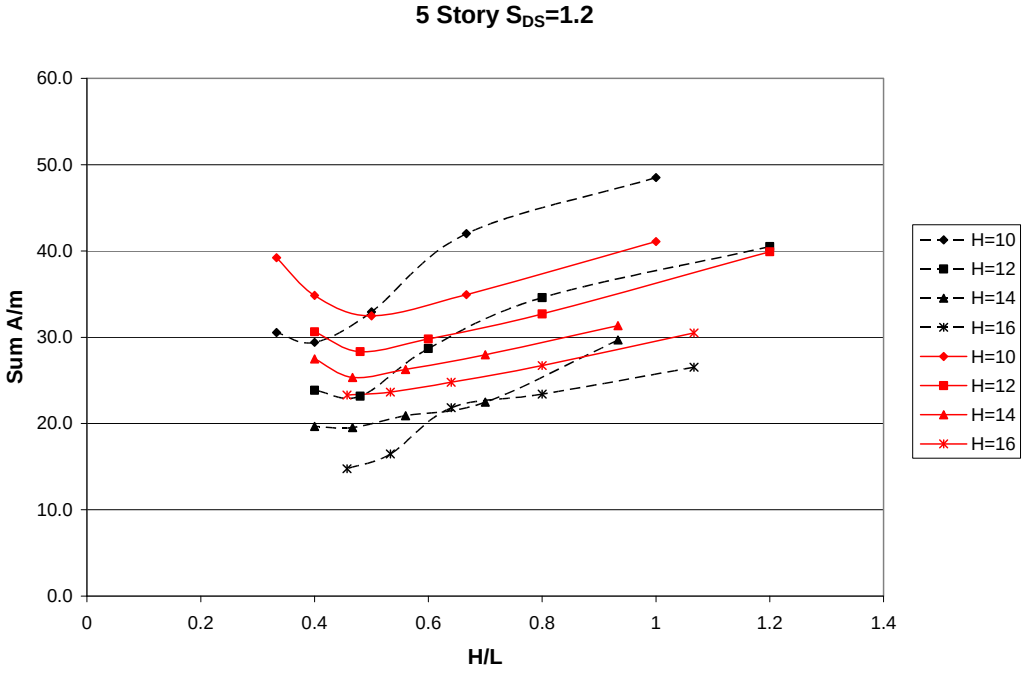

Figure 6-7 Five-Story S_{DS}=1.2 A/m

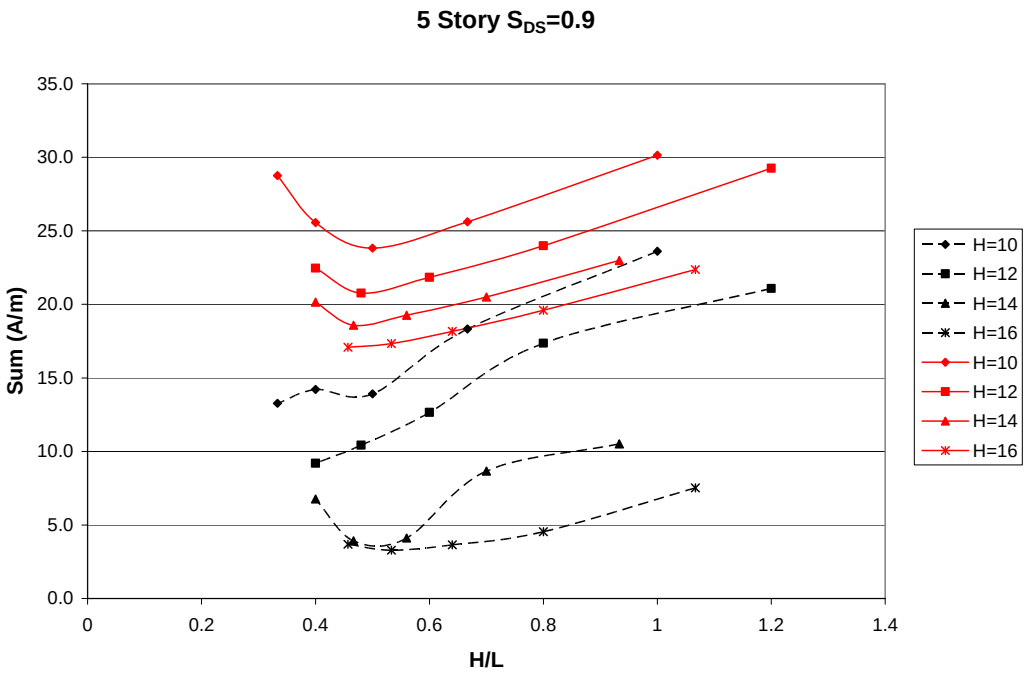

Figure 6-8 Five-Story S_{DS}=0.9 A/m

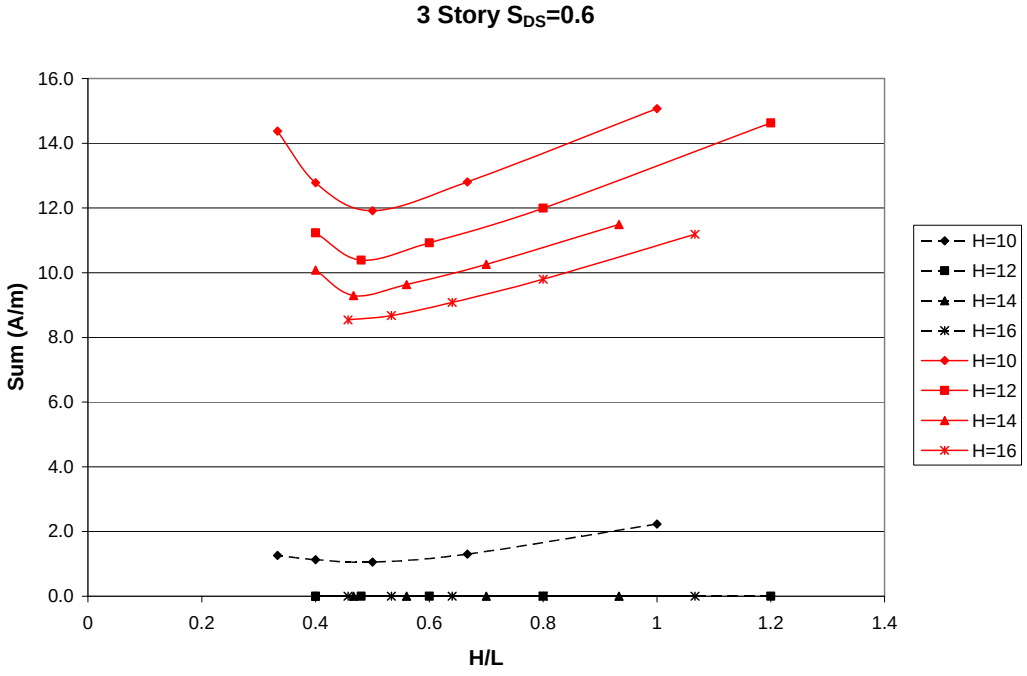

Figure 6-9 Five-Story S_{DS}=0.6 A/m

For one-story BRBF's at severe seismic loading the brace A/m determined by the ELF procedure is unconservative for almost all story heights and bay widths. For three-story and five-story BRBF's at severe seismic loading the sum of brace A/m given from the ELF procedure is unconservative for frames with small story heights and bay widths.

The brace A/m or sum of A/m calculated by ELF procedure at low seismic loading becomes excessively conservative for one-, three-, and five-story BRBF's. The sum of brace A/m for three-story and five-story frames determined by the ELF procedure at moderate seismic loading is excessively conservative for frames with large story heights and bay widths.

The optimum brace A/m determined by the NTHO procedure at low seismic loading goes to zero for BRBF's with larger story heights and bay widths. This occurs because the braces become very flexible at low seismic loading causing the fundamental period of the frame to increase until the brace area becomes zero. The ELF procedure prevents this from occurring for frames under low seismic loading by placing an upper limit on the fundamental period of the structure. Frames in regions of low seismicity are normally controlled by wind loading rather than seismic loading.

The brace A/m for one-story BRBF's designed by the ELF procedure are a function of H/L only because the graphs for different heights line up on top of each other. Also, for three-story frames the sum of brace A/m determined by the ELF procedure at severe and moderate seismic loadings is mostly a function of H/L. This is because when the fundamental period falls on the flat part of the design spectrum (between T_o and T_s), the value of the seismic coefficient Cs is constant, and therefore, independent of story height. This implies that all of the one-story BRBF's in this study have fundamental

periods between T_o and T_s. As the fundamental period exceeds the value of T_s on the response spectrum, the brace areas determined by the ELF procedure become a function of both story height and bay width. The brace areas designed by the NTHO procedure are always a function of both story height and bay width.

6.2 Controlling Constraint Tables

Drift and yielding are the two constraints that determine the brace area. Tables 6-1 through 6-9 indicate the governing constraint for the ELF and NTHO procedures for BRBF's of different story heights, bay widths, number of stories, and seismic loadings. The first word in each cell represents the governing constraint for the NTHO procedure and the second word represents the governing constraint for the ELF procedure. When drift governs then "Drift" is written in the cell. When yielding governs then "Yield" is written in the cell. For cases where the brace area goes to zero, it cannot be determined what constraint governs, and "Zero" is written in the cell. Bolded cells indicate cases when the controlling constraints differ for the two procedures.

Table 6-1 One-Story S_{DS}=1.2

	NTHO/ELF	NTHO/ELF	NTHO/ELF	NTHO/ELF
	H=10'	H=12'	H=14'	H=16'
L=10'	Yield/Yield	Yield/Yield	-	-
L=15'	Yield/Yield	Yield/Yield	Yield/Yield	Yield/Yield
L=20'	Yield/Yield	Yield/Yield	Yield/Yield	Yield/Yield
L=25'	Drift/Drift	Yield/Yield	Yield/Yield	Yield/Yield
L=30'	Drift/Drift	Drift/Drift	Yield/Yield	Yield/Yield
L=35'	-	-	Yield/Yield	Yield/Yield

Table 6-2 One-Story S_{DS}=0.9

	NTHO/ELF	NTHO/ELF	NTHO/ELF	NTHO/ELF
	H=10'	H=12'	H=14'	H=16'
L=10'	Yield/Yield	Yield/Yield	-	-
L=15'	Yield/Yield	Yield/Yield	Yield/Yield	Yield/Yield
L=20'	Yield/Yield	Yield/Yield	Yield/Yield	Yield/Yield
L=25'	Drift/Drift	Yield/Yield	Yield/Yield	Yield/Yield
L=30'	Drift/Drift	Drift/Drift	Yield/Yield	Yield/Yield
L=35'	-	-	Yield/Yield	Yield/Yield

Table 6-3 One-Story S_{DS}=0.6

	NTHO/ELF	NTHO/ELF	NTHO/ELF	NTHO/ELF
	H=10'	H=12'	H=14'	H=16'
L=10'	Yield/Yield	Yield/Yield	-	-
L=15'	Yield/Yield	Yield/Yield	Yield/Yield	Yield/Yield
L=20'	Yield/Yield	Yield/Yield	Yield/Yield	Yield/Yield
L=25'	Drift/Drift	Yield/Yield	Yield/Yield	Yield/Yield
L=30'	**Zero/Drift**	**Zero/Drift**	Yield/Yield	**Zero/Yield**
L=35'	-	-	**Zero/Yield**	**Zero/Yield**

Table 6-4 Three-Story S_{DS}=1.2

	NTHO/ELF	NTHO/ELF	NTHO/ELF	NTHO/ELF
	H=10'	H=12'	H=14'	H=16'
L=10'	Yield/Yield	Yield/Yield	-	-
L=15'	Yield/Yield	Yield/Yield	Yield/Yield	Yield/Yield
L=20'	Yield/Yield	Yield/Yield	Yield/Yield	Yield/Yield
L=25'	Yield/Yield	Yield/Yield	Yield/Yield	Yield/Yield
L=30'	Drift/Drift	Yield/Yield	Yield/Yield	Yield/Yield
L=35'	-	-	Yield/Yield	Yield/Yield

Table 6-5 Three-Story S_{DS}=0.9

	NTHO/ELF	NTHO/ELF	NTHO/ELF	NTHO/ELF
	H=10'	H=12'	H=14'	H=16'
L=10'	Yield/Yield	Yield/Yield	-	-
L=15'	Yield/Yield	Yield/Yield	Yield/Yield	Yield/Yield
L=20'	Yield/Yield	Yield/Yield	Yield/Yield	Yield/Yield
L=25'	Yield/Yield	Yield/Yield	Yield/Yield	Yield/Yield
L=30'	Drift/Drift	Yield/Yield	Yield/Yield	Yield/Yield
L=35'	-	-	Yield/Yield	Yield/Yield

Table 6-6 Three-Story S_{DS}=0.6

	NTHO/ELF	NTHO/ELF	NTHO/ELF	NTHO/ELF
	H=10'	H=12'	H=14'	H=16'
L=10'	Yield/Yield	Yield/Yield	-	-
L=15'	Yield/Yield	Yield/Yield	Yield/Yield	**Zero/Yield**
L=20'	Yield/Yield	Yield/Yield	Yield/Yield	**Zero/Yield**
L=25'	Yield/Yield	Yield/Yield	**Zero/Yield**	**Zero/Yield**
L=30'	Drift/Drift	**Zero/Yield**	**Zero/Yield**	**Zero/Yield**
L=35'	-	-	**Zero/Yield**	**Zero/Yield**

Table 6-7 Five-Story S_{DS}=1.2

	NTHO/ELF	NTHO/ELF	NTHO/ELF	NTHO/ELF
	H=10'	H=12'	H=14'	H=16'
L=10'	Yield/Yield	Yield/Yield	-	-
L=15'	Yield/Yield	Yield/Yield	Yield/Yield	Yield/Yield
L=20'	**Drift/Yield**	Yield/Yield	Yield/Yield	Yield/Yield
L=25'	Drift/Drift	**Drift/Yield**	Yield/Yield	Yield/Yield
L=30'	Drift/Drift	Drift/Drift	Drift/Drift	**Drift/Yield**
L=35'	-	-	Drift/Drift	Drift/Drift

Table 6-8 Five-Story S_{DS}=0.9

	NTHO/ELF	NTHO/ELF	NTHO/ELF	NTHO/ELF
	H=10'	H=12'	H=14'	H=16'
L=10'	Yield/Yield	Yield/Yield	-	-
L=15'	Yield/Yield	Yield/Yield	Yield/Yield	Yield/Yield
L=20'	**Drift/Yield**	Yield/Yield	Yield/Yield	Yield/Yield
L=25'	Drift/Drift	**Drift/Yield**	Yield/Yield	Yield/Yield
L=30'	Drift/Drift	Drift/Drift	Drift/Drift	**Drift/Yield**
L=35'	-	-	Drift/Drift	Drift/Drift

Table 6-9 Five-Story S_{DS}=0.6

	NTHO/ELF	NTHO/ELF	NTHO/ELF	NTHO/ELF
	H=10'	H=12'	H=14'	H=16'
L=10'	Yield/Yield	**Zero/Yield**	-	-
L=15'	Yield/Yield	**Zero/Yield**	**Zero/Yield**	**Zero/Yield**
L=20'	**Drift/Yield**	**Zero/Yield**	**Zero/Yield**	**Zero/Yield**
L=25'	Drift/Drift	**Zero/Yield**	**Zero/Yield**	**Zero/Yield**
L=30'	Drift/Drift	**Zero/Drift**	**Zero/Drift**	**Zero/Yield**
L=35'	-	-	**Zero/Drift**	**Zero/Drift**

Except for cases where the NTHO goes to zero brace area, the governing constraints for the ELF and NTHO procedures are the same for all BRBF's except for three different five-story BRBF's. The three five-story BRBF,s have different controlling constraints because the ELF procedure is more conservative with regard to yield failure in these cases.

6.3 Design Charts

Design charts were successfully constructed using the NTHO procedure. The design charts found in Figures 6-10 through 6-32 represent BRBF's with different story heights, bay widths, number of stories, and seismic levels. The design charts determine BRBF brace area at each story. To use these design charts one first needs the story height, bay width, number of stories, seismic level, and the mass per story. The design charts are limited to structures that have the same mass at each story, the same height for each story, and the same width for each braced bay. There are no design charts for three-story and five-story BRBF's where the brace areas go to zero (low seismicity). It is assumed that wind design charts are needed for these frames.

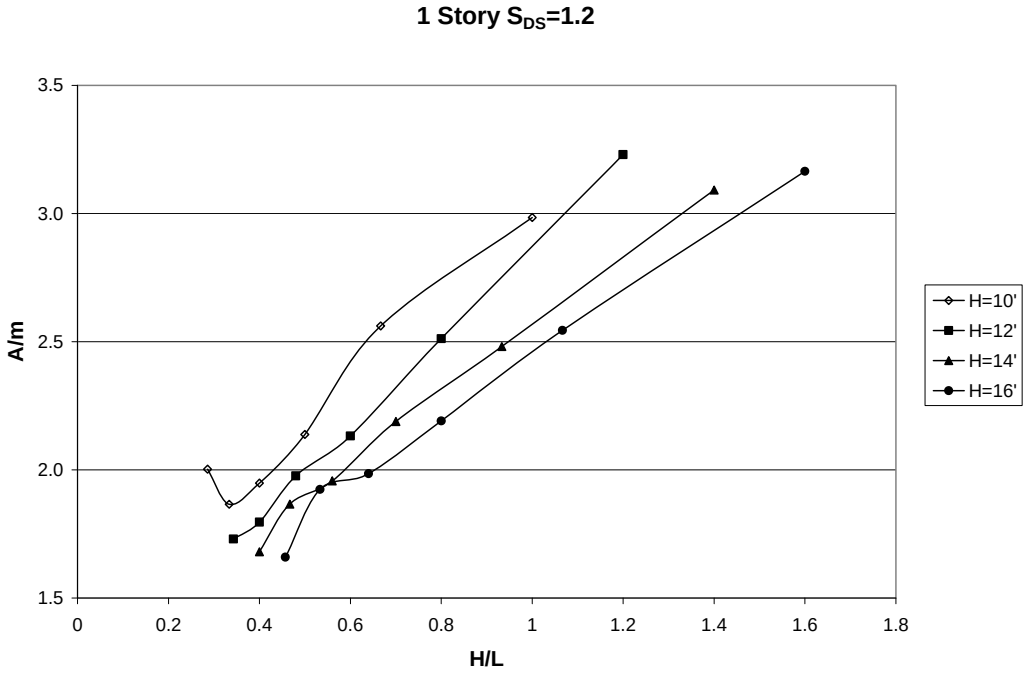

Figure 6-10 One-Story Design Chart

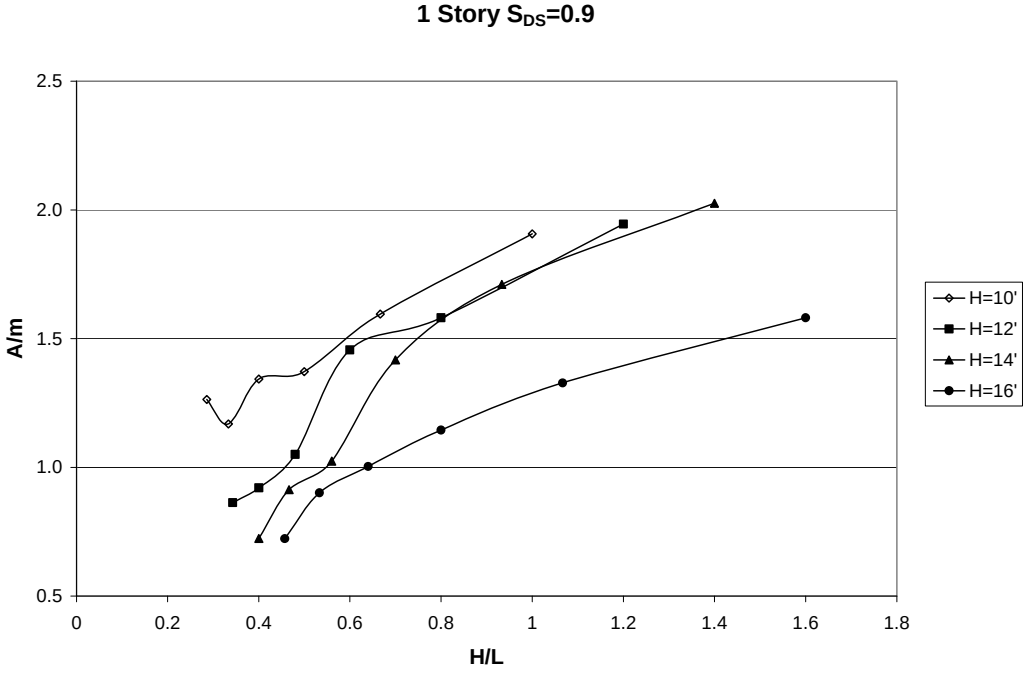

Figure 6-11 One-Story Design Chart

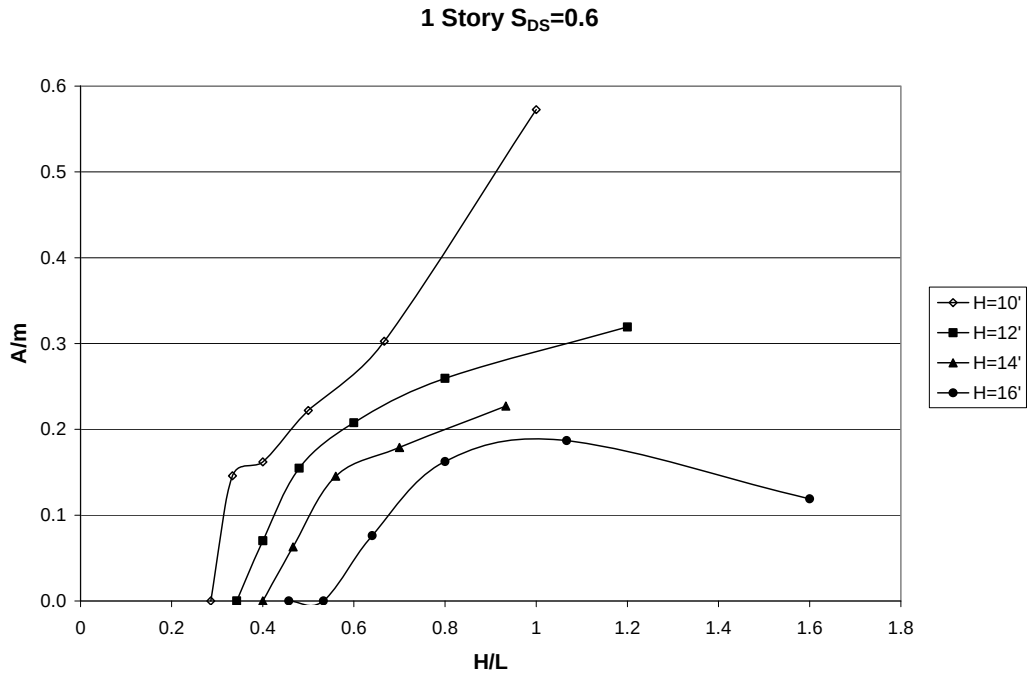

Figure 6-12 One-Story Design Chart

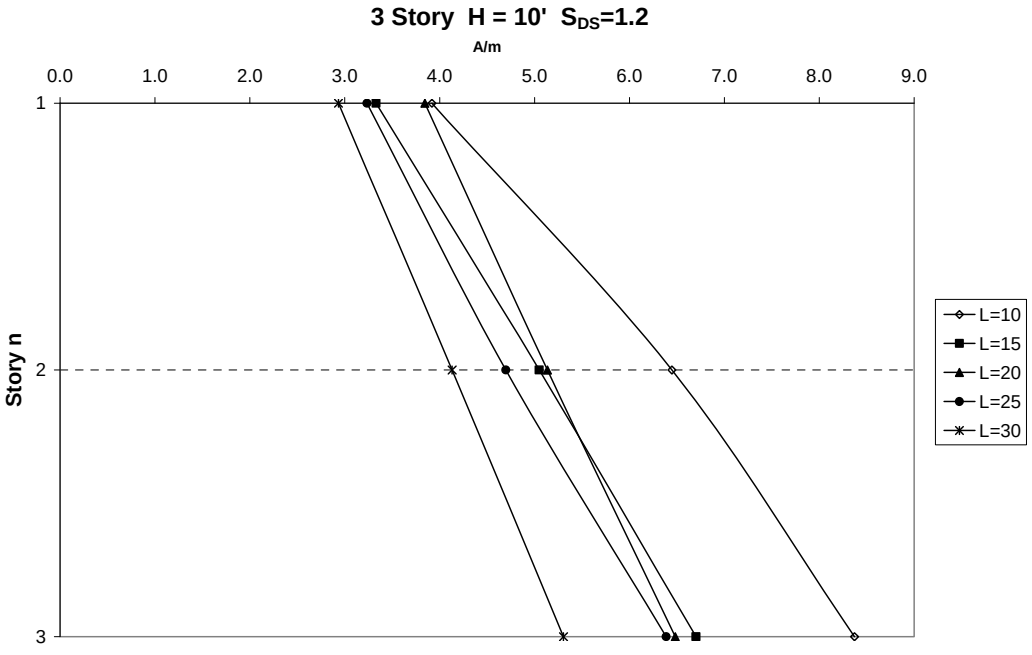

Figure 6-13 Three-Story Design Chart

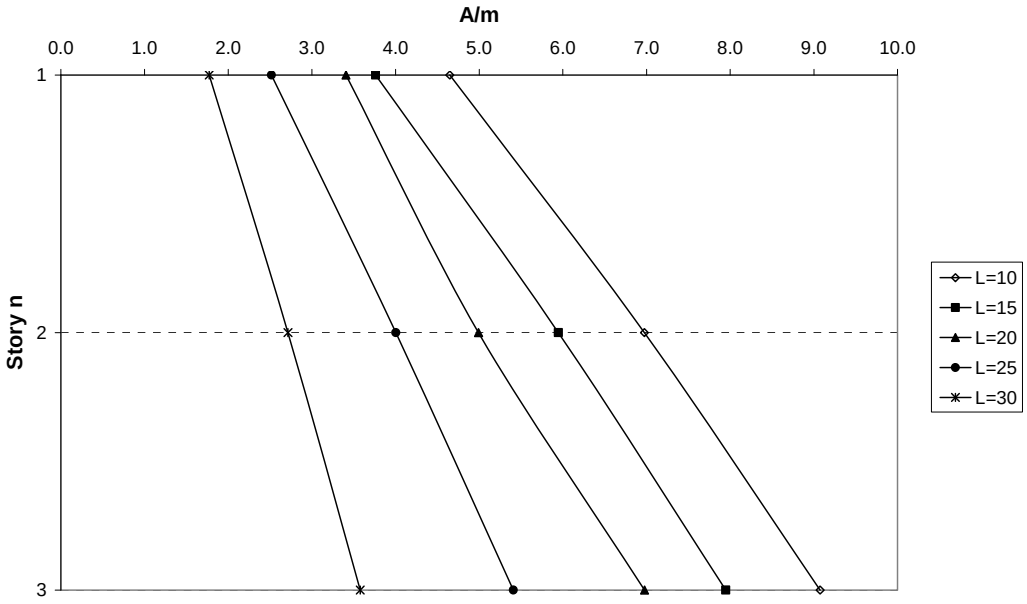

Figure 6-14 Three-Story Design Chart

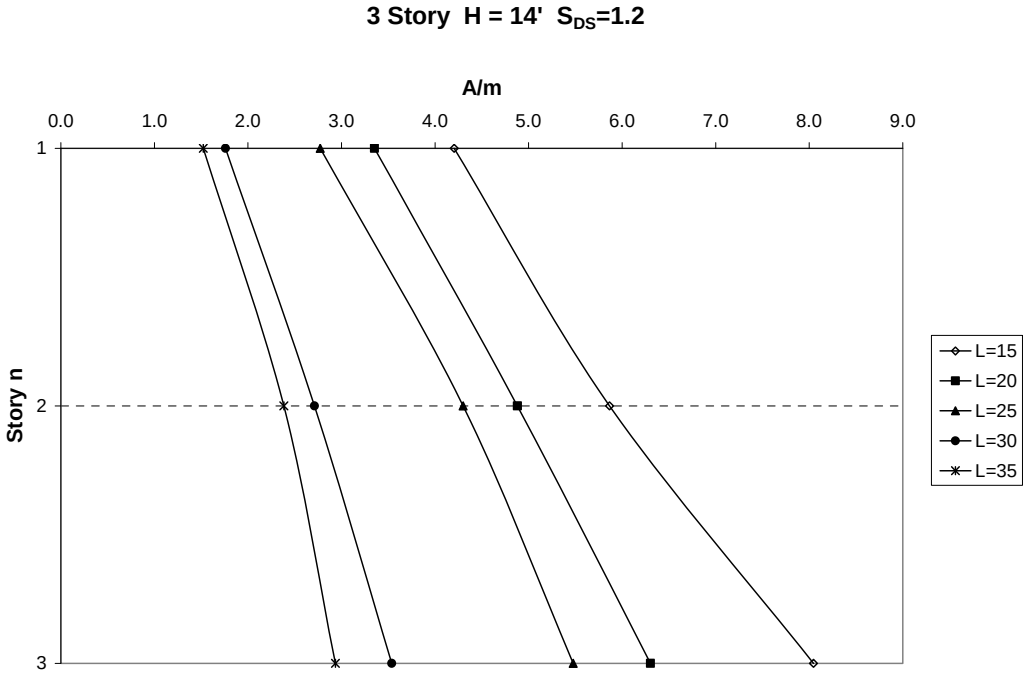

Figure 6-15 Three-Story Design Chart

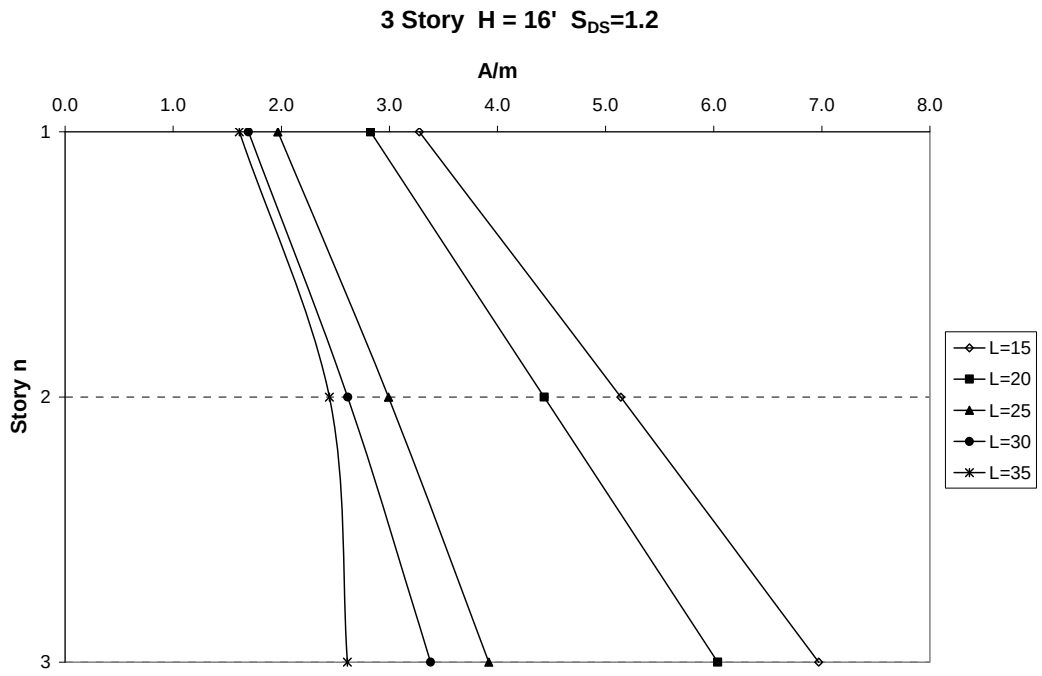

Figure 6-16 Three-Story Design Chart

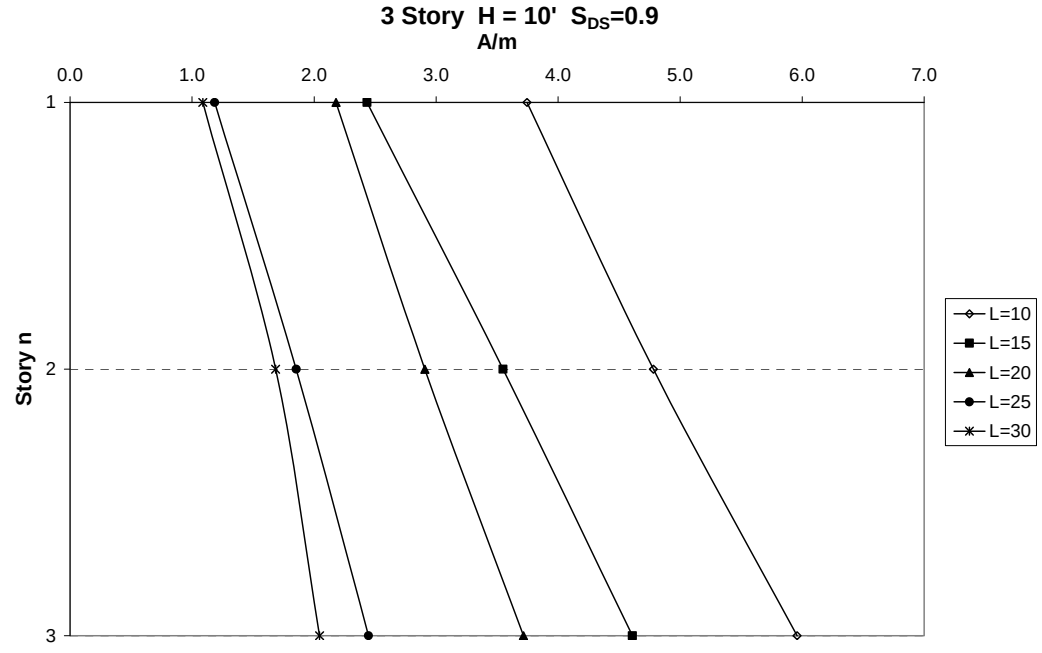

Figure 6-17 Three-Story Design Chart

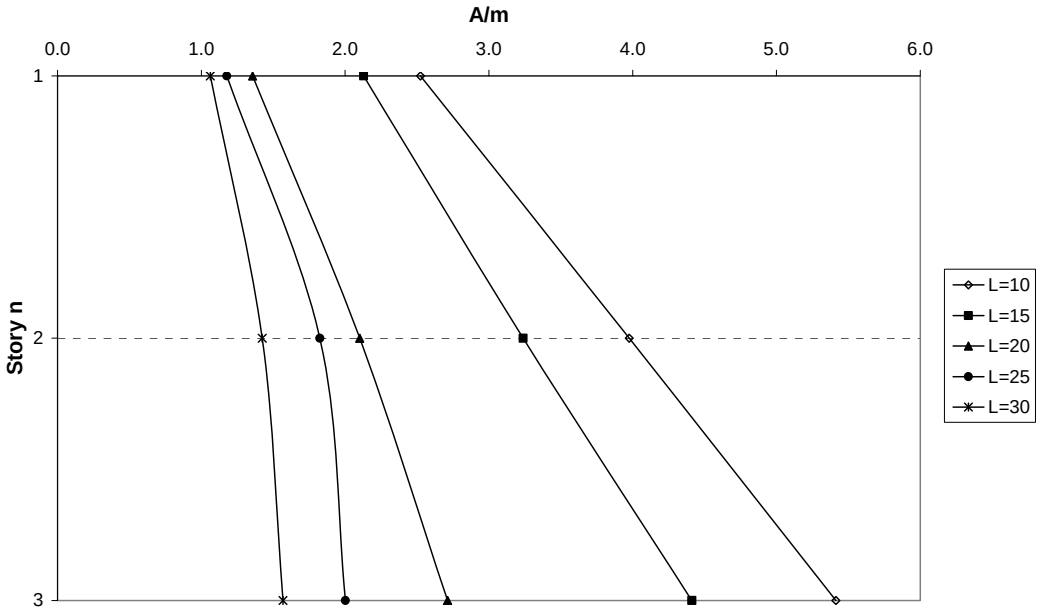

Figure 6-18 Three-Story Design Chart

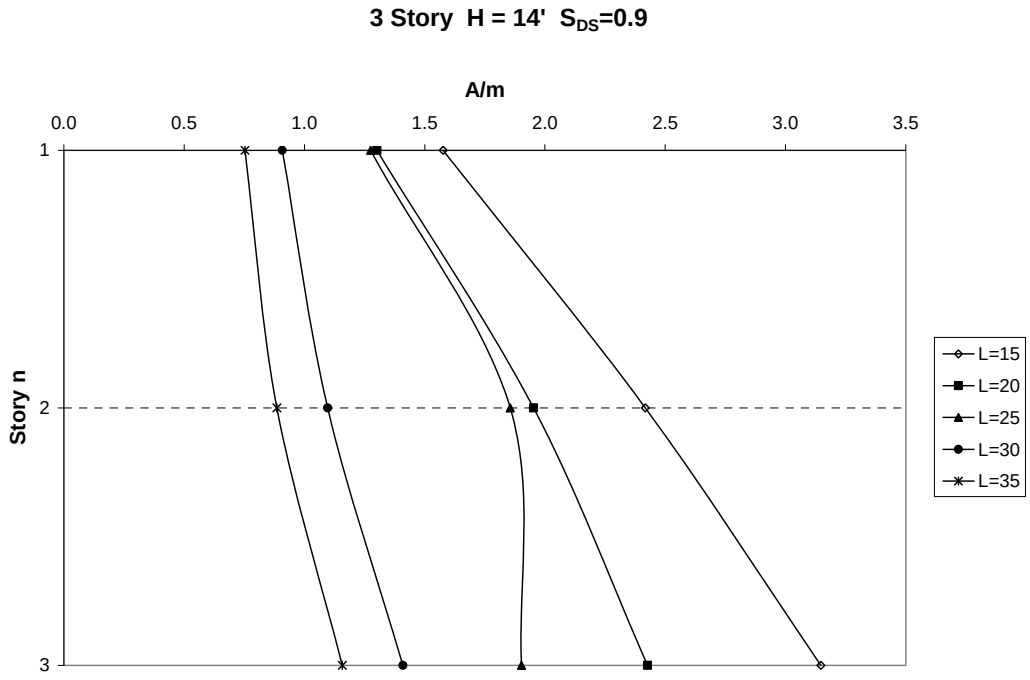

Figure 6-19 Three-Story Design Chart

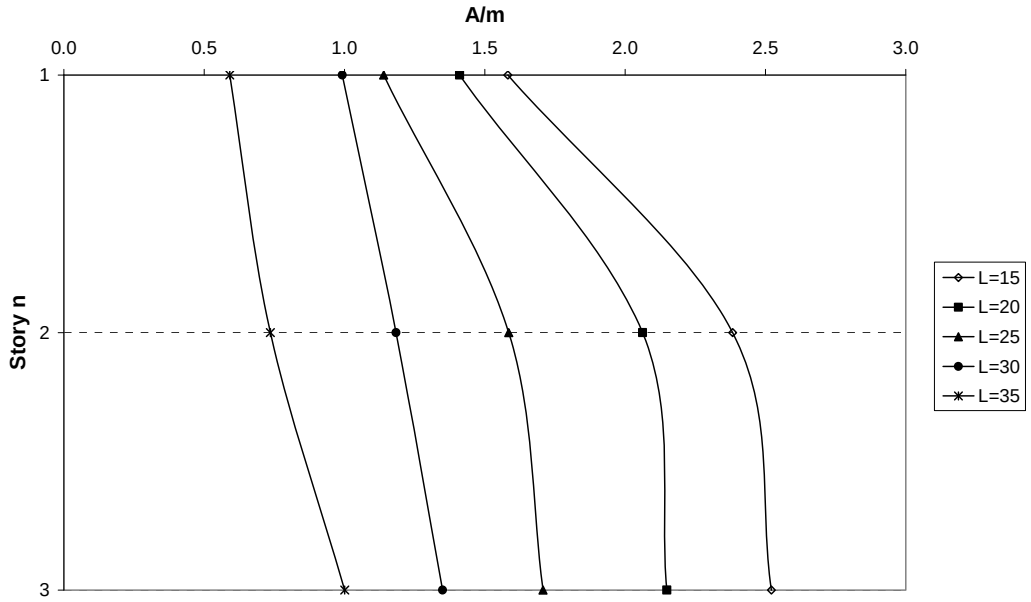

Figure 6-20 Three-Story Design Chart

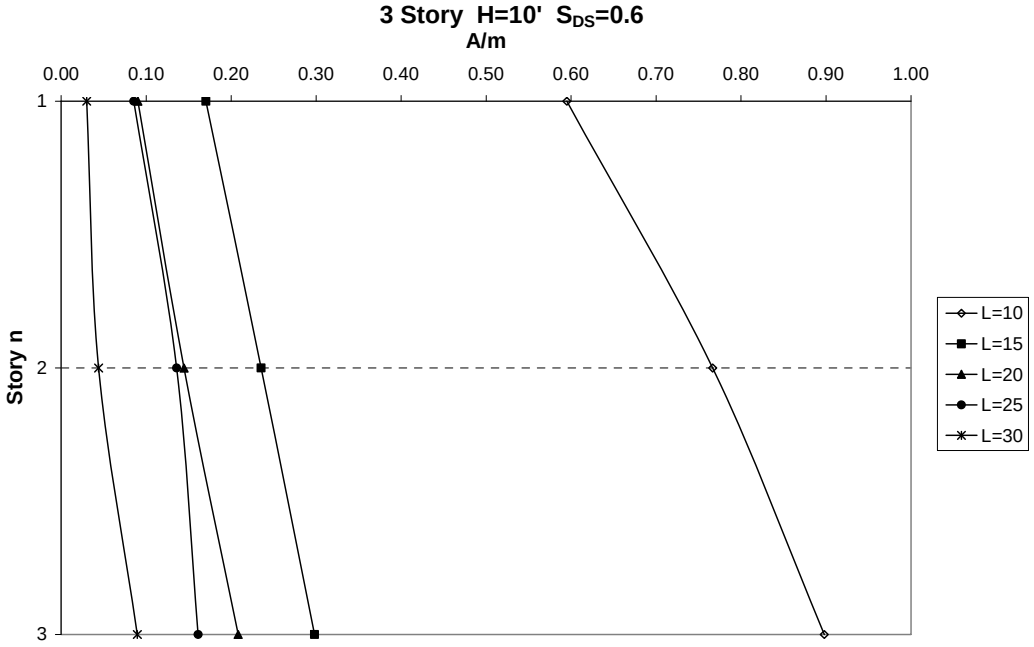

Figure 6-21 Three-Story Design Chart

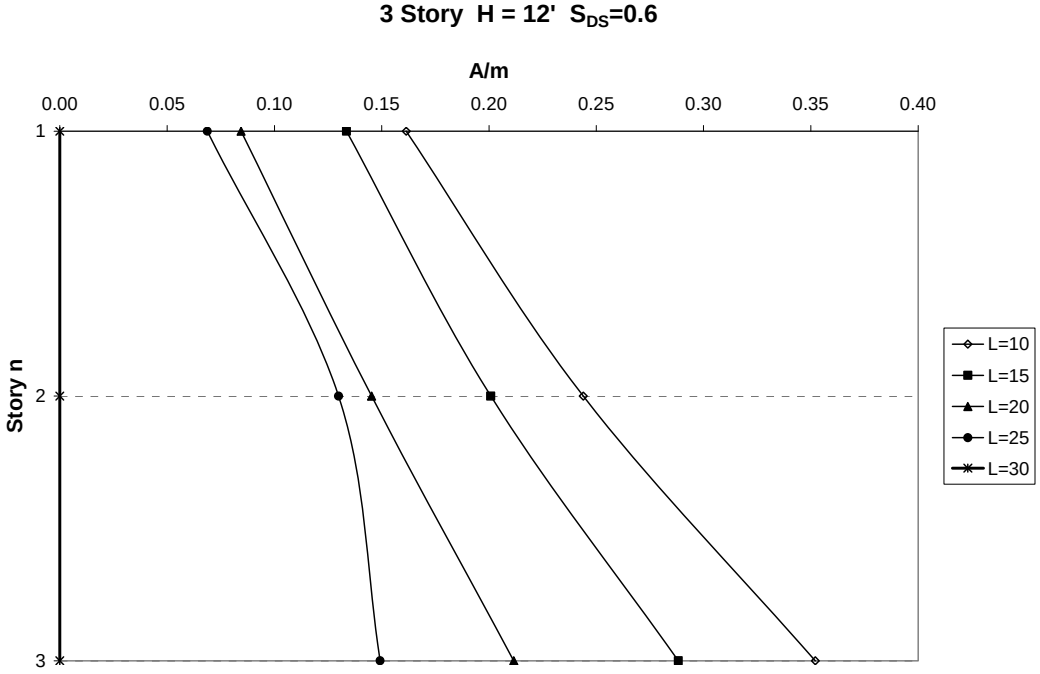

Figure 6-22 Three-Story Design Chart

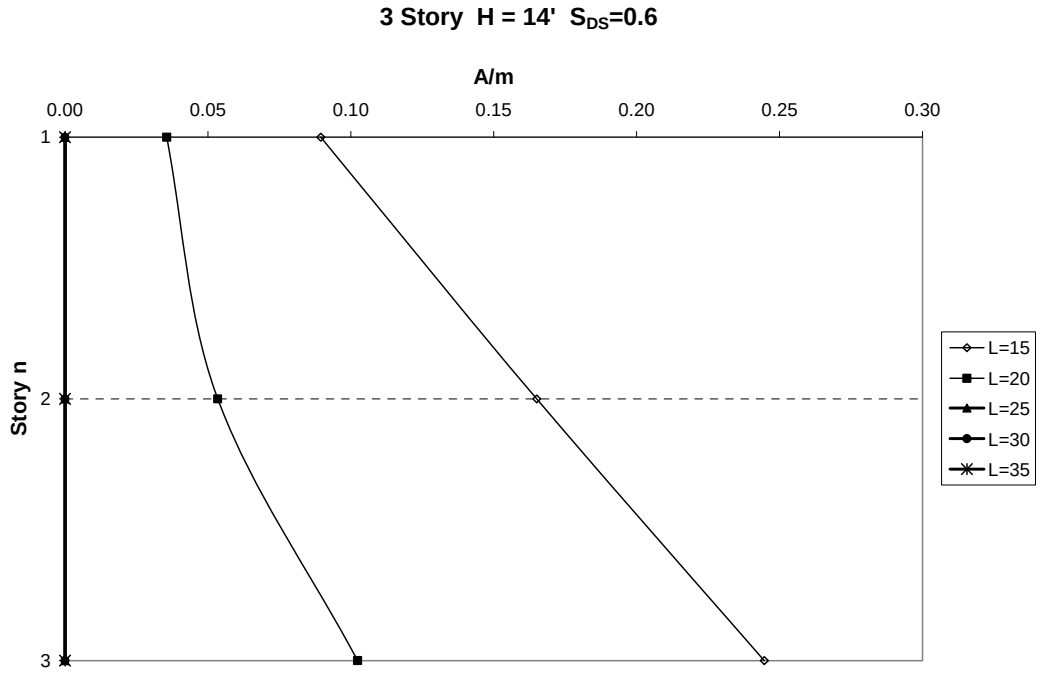

Figure 6-23 Three-Story Design Chart

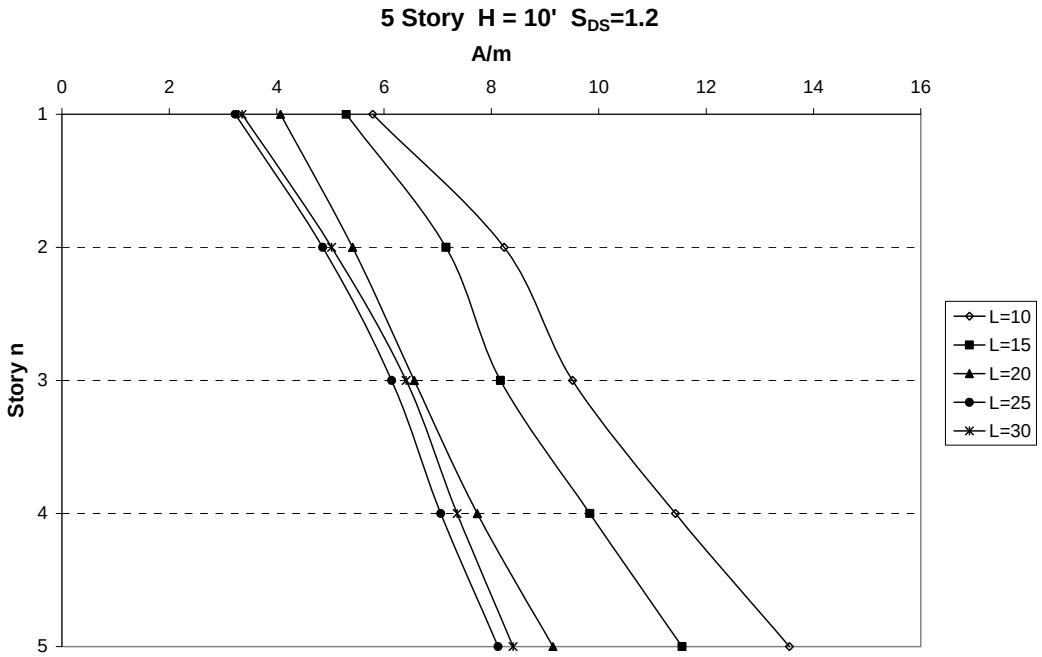

Figure 6-24 Five-Story Design Chart

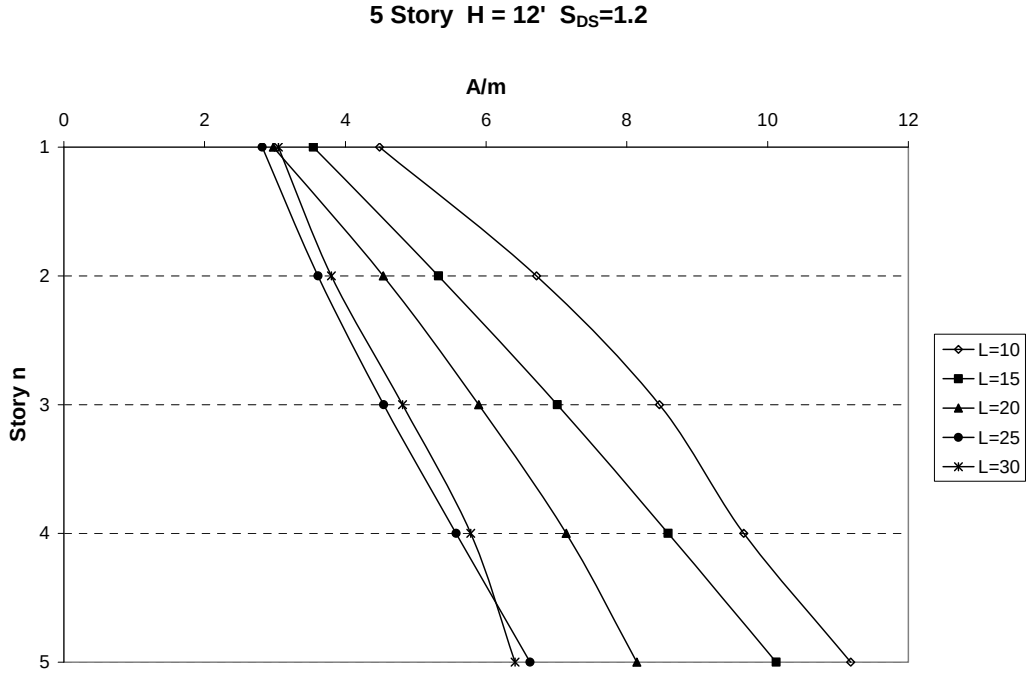

Figure 6-25 Five-Story Design Chart

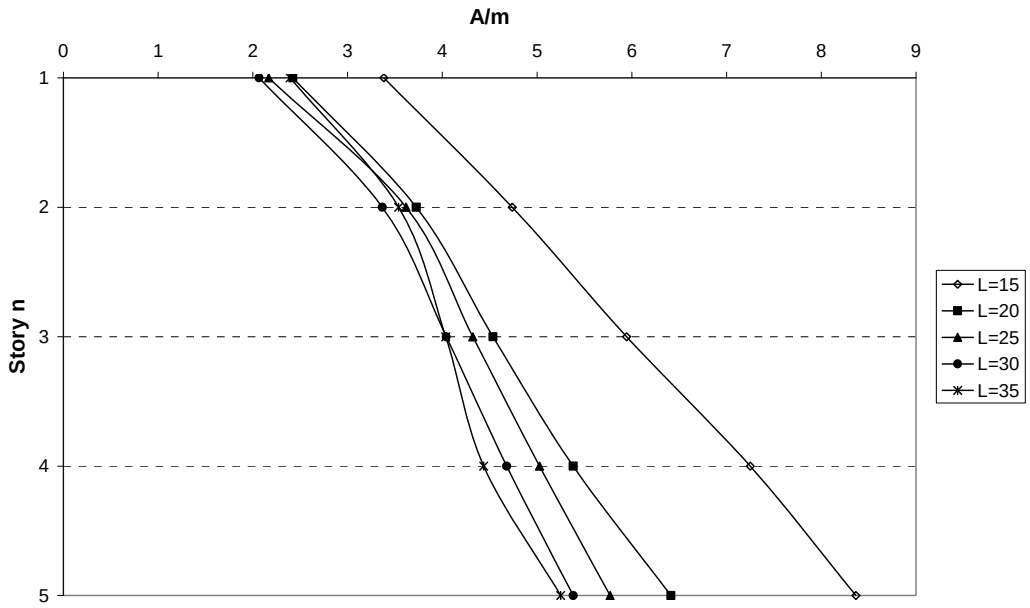

Figure 6-26 Five-Story Design Chart

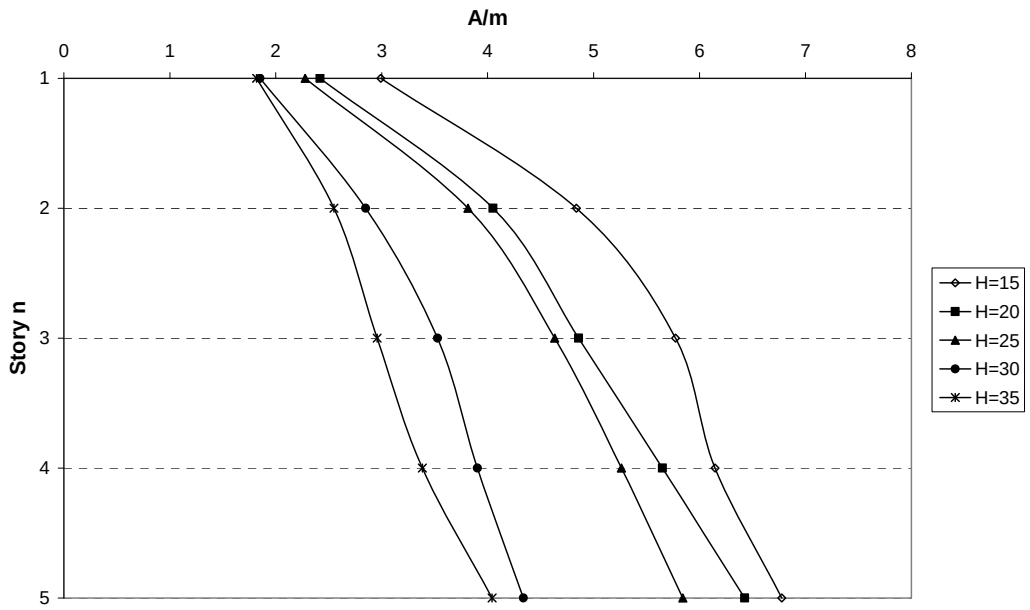

Figure 6-27 Five-Story Design Chart

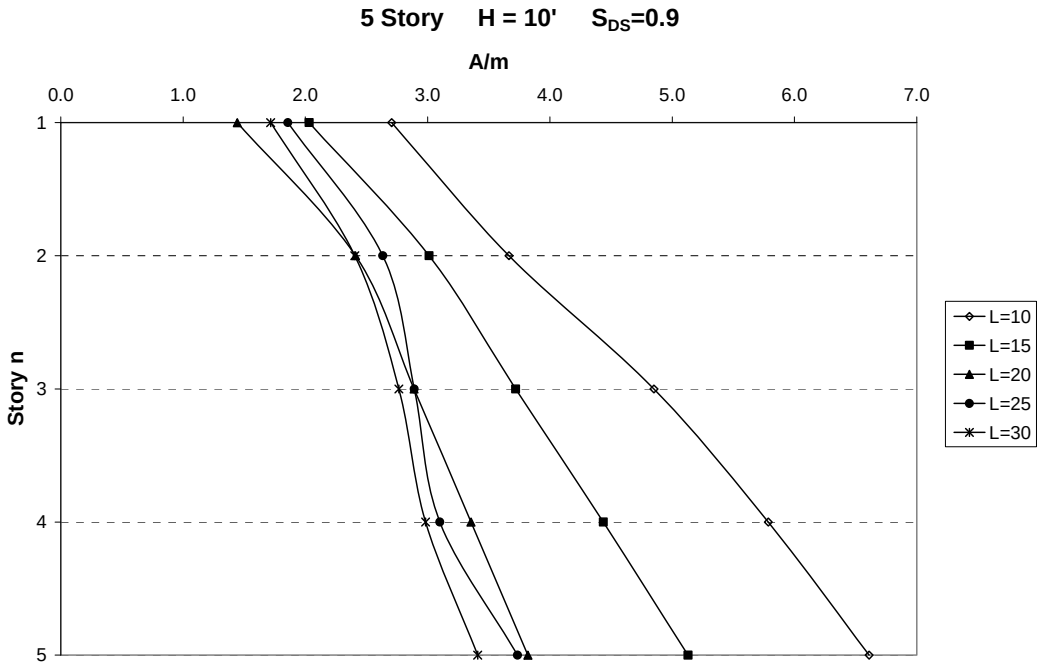

Figure 6-28 Five-Story Design Chart

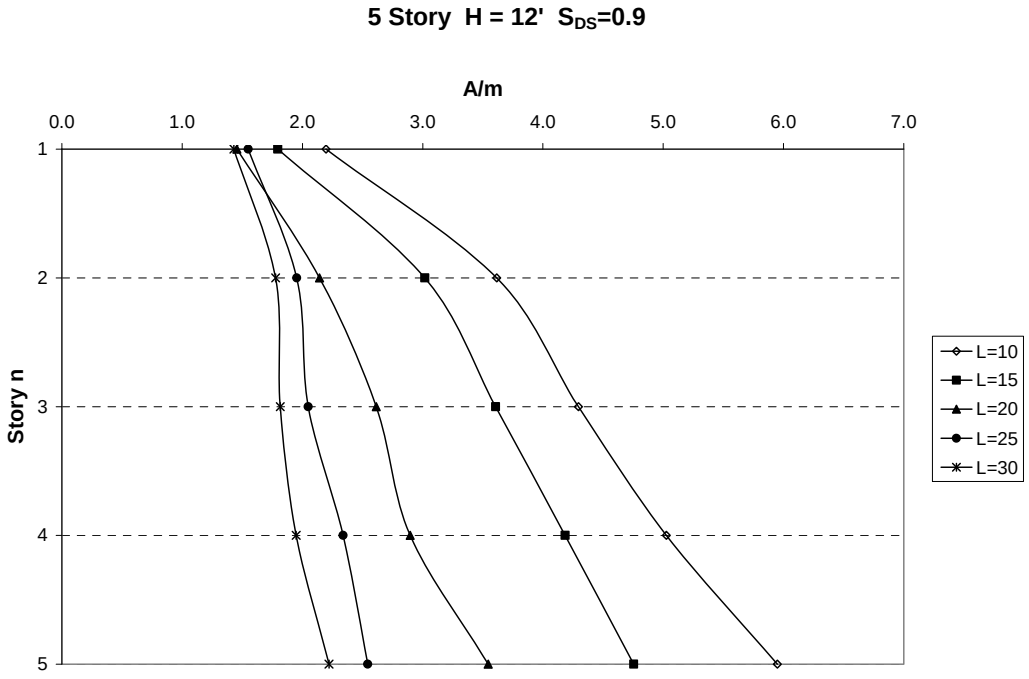

Figure 6-29 Five-Story Design Chart

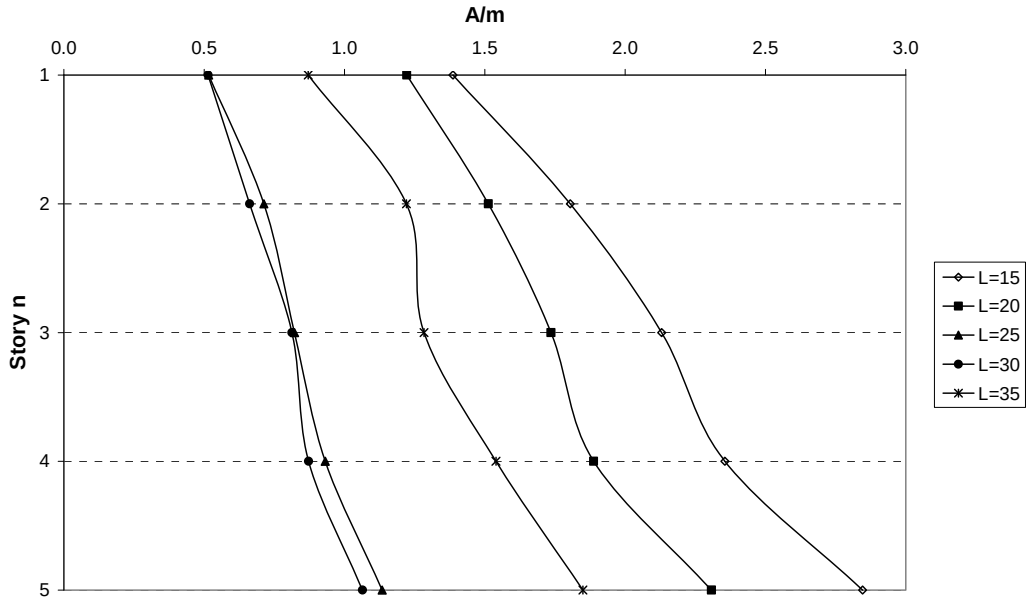

Figure 6-30 Five-Story Design Chart

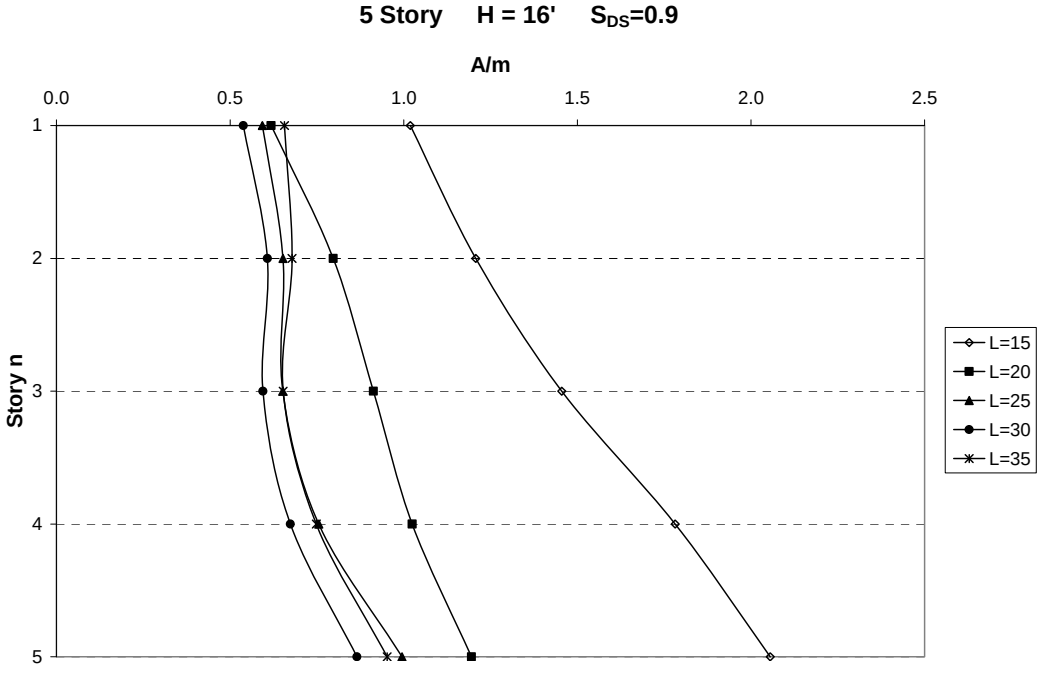

Figure 6-31 Five-Story Design Chart

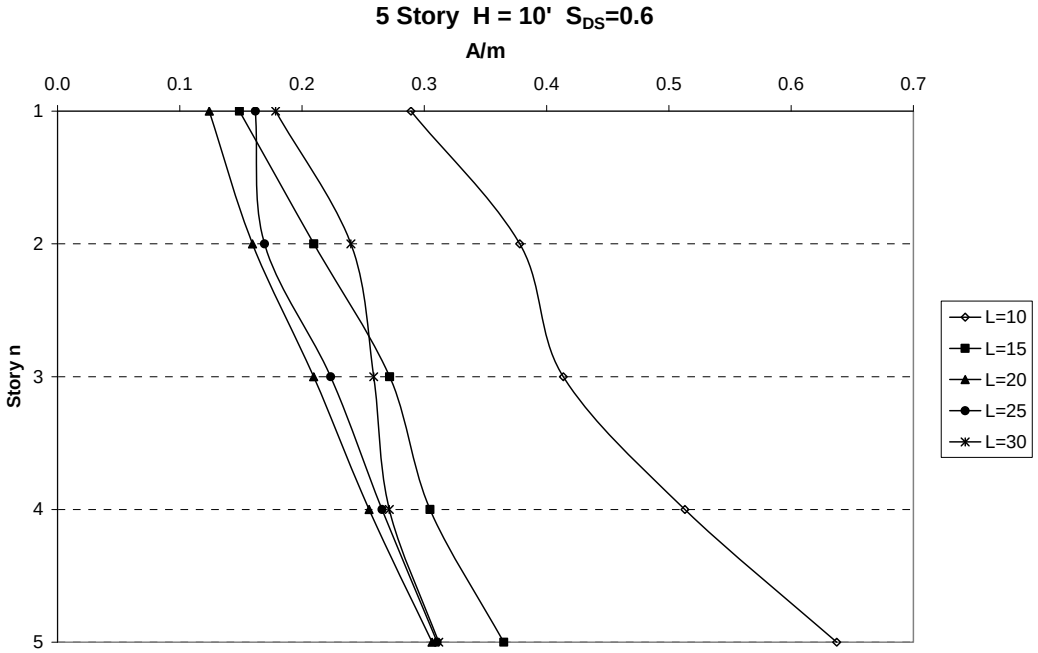

Figure 6-32 Five-Story Design Chart

An unexpected result from the NTHO procedure is the near linearity of the variation of A/m from story to story for most multistory BRBF's. Although not shown, this is not the case for the ELF procedure.

7 Conclusion

The NTHO procedure was successfully developed for the design of BRBF's, and results were compared with those produced by the ELF procedure. Design charts were successfully created using results from the NTHO procedure. Therefore, all three research goals, as stated in the introduction, were achieved. Conclusions were made in the previous chapter and are summarized below:

1) Brace areas from the ELF procedure are unconservative for severe seismic loading acting on one-story BRBF's and on multi-story BRBF's with short story heights and bay widths.
2) Brace areas from the ELF procedure are excessively conservative for moderate and low seismic loading acting on multi-story BRBF's.
3) Optimum brace areas determined by the NTHO procedure may go to zero for low seismic loading acting on BRBF's with large story heights and bay widths.
4) Brace areas are a function of H/L for one-story frames designed by the ELF procedure.
5) The controlling constraints for the two procedures differ only for a few five-story frames

6) Brace areas determined by the NTHO procedure vary linearly from story to story, which is not the case for brace areas determined by the ELF procedure.

One recommendation is to further expand the design charts that were developed in this research to more BRBF's. This would include BRBF's with varying mass and height from story to story. It is also recommended that the design charts be supplemented with wind design criteria for areas of low siesmicity. In addition, a computer program could be provided using the NTHO procedure for special BRBF's that fall outside the application of the design charts.

Finally, it is also recommended that the ELF procedure be revised for BRBF's where this research has shown that it is unconservative or excessively conservative. The ELF procedure should also be modified so that final brace areas vary linearly from story to story.

References

AISC (2005), AISC 341, Seismic provisions for structural steel buildings, American Institute of Steel Construction Inc., Chicago, IL

ASCE (2005), ASCE 7-05, Minimum design loads for buildings and other structures, American Society of Civil Engineering, Reston, VA

Black, C., and Makris, N. (2004). "Component testing, seismic evaluation and characterization of buckling-restrained braces." *J. Structural Engineering*, 130(6), 880-894

Chopra, A. K. (1995), Dynamics of structures: theory and application to earthquake engineering, Prentice-Hall, Englewood Cliffs, NJ

Coy, B. B. (2007). "Buckling-restrained brace connection design and testing." Unpublished masters thesis, Brigham Young University, Provo, UT.

FEMA (2003), NEHRP recommended provisions for seismic regulations for new buildings and other structures FEMA 450, Federal Emergency Management Agency, Washington, DC

Hayalioglu, M. S., & Degertekin, S. O. (2004). Design of non-linear steel frames for stress and displacement constraints with semi-rigid connections via genetic optimization. *Structural and Multidisciplinary Optimization, 27*(4), 259-271.

Kameshki, E. S., and Saka, M.P. (2001). "Genetic algorithm based optimum bracing design of non-swaying tall plane frames." J. Constructional Steel Research, 57(10), 1081-1097

Kiggins, S., & Uang, C. (2006). Reducing residual drift of buckling-restrained braced frames as a dual system. *Engineering Structures, 28*(11), 1525-1532.

Kim, J., and Choi, H. (2004). "Behavior and design of structures with buckling-restrained braces." Engineering structures, 26(6), 693-706

Kim, J., and Seo, Y. (2004). "Seismic design of low-rise steel frames with buckling-restrained braces." *Engineering structures*, 26(5), 543-551

3 spaces before and after figures/tables and their caption

Memari, A. M., and Madhkhan, M. (1999). "Optimal design of steel frames subject to gravity and seismic codes' prescribed lateral forces." *Structural Optimization*, 18(1), 55-66

Tests of Nippon Steel Corporation Unbonded Braces" - A Report to: Ove Arup & Partners California, Ltd submitted by Nippon Steel Corporation, Tokyo, Japan, prepared by SIE Corporation, July 2, 1999.

Pezeshk S. (1998), "Design of framed structures: an integrated non-linear analysis and optimal minimum weight design." *Int. J. Numerical Methods in. Engng*., 41, 459-471

Pezeshk S., and Camp, C. V. (2000). "Design of nonlinear framed structures using genetic optimization." *J. Structural Engineering*, 126(3), 387-388

Sabelli, R., Mahin, S. and Chang, C. (2003). "Seismic demand on steel braced frame buildings with buckling-restrained braces." *Engineering Structures*, 25(5), 655-666

Sabelli, R., and Pottebaum, W. (2005) "Design of a buckling-restrained braced frame utilizing 2005 seismic standards." *Proceedings of the Structures Congress and Exposition, Metropolis and Beyond - Proceedings of the 2005 Structures Congress and the 2005 Forensic Engineering Symposium*, 1807-1818

SEAOC (1999), *Recommended Lateral Force Requirements and Commentary* (SEAOC Blue Book). ICBO: Whittier, CA

Trembley, R., and Buldoc, P. (2006). "Seismic testing and performance of buckling-restrained bracing systems." *Canadian J. Civil Engineering*, 33(2), 183-198

Watanabe, A., and Hitomoi, Y. (1988). "Properties of braces encased in buckling restraining concrete and steel tube." *Proceedings of the 10th World Conference on Earthquake Engineering,* Tokyo-Kyoto, Japan

Xu, L., Gong, Y., & Grierson, D. E. (2006). Seismic design optimization of steel building frameworks. *Journal of Structural Engineering, 132*(2), 277-286